Reviewers' Comments:

Reviewer #1:
Remarks to the Author:
The manuscript of Garcia Lopez et al describes the identification of a small molecule (PK4C9) as a modulator of SMN exon 7 splicing through its interaction with the TSL2 RNA loop located on the 5'ss of exon 7. The data is well described and the authors present a thorough study of the mechanism of action of PK4C9.

Specific comments are as follows:

1- In Fig 1b the visual estimation of the intensity of the western bands not always match with the scanning data presented in Fig 1c. In particular for the mutant TSL2 4G (5th lane). In fact, while in the western I would guess is even less E7 inclusion that in the SMN 2 TSL2nm (second lane) in the scanning appears slightly higher. An inconsistency between western and scan may also be present with the mutant 9C.
In Fig 1e the meaning of "others" should be explained in the figure legend

2- Page 5 lines 112-114 The authors interpret the effect of the 4G mutation in structural terms, they should discuss also the possibility of creating a splicing factor binding site that in turn inhibits splicing of exon 7 independently of the structure. The 4G mutation seems to expose a sequence GUAAGGAGU that although not fully "canonical" could be a binding site of hnRNPA1 or other proteins of that family whose binding will in turn hamper 5'ss recognition

3- Minor point, there is a typo in Page 7 line 148 TSL2-interacting

4- Fig 3e and Page 7 lines 170-176: The authors should comment on the fact that in Drosophila the SMN2 gene exon 7 seems to be included in a very high percentage (72%?). In fact exclusion of exon7 is barely visible before PK4C9 treatment

5- Fig 4a and Page8 lines 182-187: It is surprising that with the almost total restoration of normal exon 7 inclusion at the RNA level (Fig 3b and 3c) there is such a marginal increase in protein as seen by western blot. The recovery of the gems (Fig 4b) is certainly impressive but a measure of the total amount of mRNA containing exon 7 before and after treatment with PK4C9 is worth doing. The qPCR tends to give overestimates of the functional intact mRNA present in the cell, a Northern blot will give a more definitive result of the mRNAs including and excluding exon 7.

6- It is not clear how the authors differentiate PK4C9 effects on splicing due to SMN recovery or to a direct off target effect of PK4C9. The eventual off target effects seen in WT fibroblasts after PK4C9 treatment should be more widely discussed particularly on the light of potential use as a therapeutic agent.

Reviewer #2:
Remarks to the Author:
In this manuscript Garcia-Lopez et al. identified a natural compound binding to the stem-loop RNA structure of SMN2 exon 7 and report a detailed characterization of the mode of action of this compound in vitro, in cells, and in drosophila. The manuscript contains a large amount of data, is technically sound, and a piece of work of high quality.
However, there are several points that need to be addressed before the manuscript is suitable for publication. This regards in particular the fact that the compound binds to the terminal ends of the stem loop structure. In the in vivo situation the terminal ends are not freely available. Is the interaction mode determined by NMR and MD compatible with this in vivo situation? From figure 6 d and 6 there seem to be only a few contacts between the natural compound and the RNA.

Wouldn't the authors expect a broad range of unspecific effects?
The NMR chemical shift perturbations shown in Figure 5d seem rather small to me given that the compound has aromatic rings. Wouldn't the authors expect larger chemical shift perturbations due to ring current effects. Do the chemical shifts back-calculated from the MD model match what they see in the spectrum? Did the authors follow the chemical shift changes of the ligand by NMR and could they validate their MD data with respect to the ligand - stem-loop RNA interactions shown in Figure 5?

Minor points:
- some figure labels are too small and hard to read, e.g. Fig. 1a numbering of nucleotides etc.
- some figures miss proper axes labels/units, e.g. Figure 1d (what is 'max'), Figure 1f (CD)
- in some figures a broken axis is shown, but there are no data points extending to these values (e.g. Fig. 1e, Fig. 1d)
- some figures miss error bars, e.g. Fig. 1d,
- Figure 3e 'Drosophila MN' is there anything missing?
- Figure 4 seems of poor resolution

Reviewer #3:
Remarks to the Author:
Garcia-Lopez et al show that one can use drugs (PK4C9 as most efficient) to rescue the reduction of SMN1 by mis-splicing, causing SMA, by induction of a secondary structure change of the isoform SMN2 becoming splicing competent at the required point. In this paper many methods are coherently represented and a comprehensive evidence based conclusion is drawn.

Most methods are standard in the field, as is most of the application. However, the detailed structural work for finding out the mechanism of drug action is unusual and brings out new information about this drug and the splicing mechanism - at least partial - some of this was already suggested at lower resolution. This work is well done and should set a standard for the field of drug development on RNA drugs - to include more detailed mechanistic studies with the completeness of methods.

Major points should be clarified:

- Line 275-277: Why is this coupling assumed? (loop formation to terminal opening) -> how is this interaction/conformational change information transported over that long distance?
- Could some of it simply be explained by less overall stability (e.g. U2A mutation) -> add melting temperatures (e.g. from Fig S2, but preferred by UV),
- Line 129-132: would that not also decrease specificity?

Some minor changes need to be addressed:

- line 114/115: what indicates the native page conclusion of hairpin formation? – more detail please (e.g. marker…)
- CD experiments: melting curves: maybe the effect is caused by difference in stability rather than conformation?
- Suppl. Table S1 is wrongly called Suppl. Table S2, Tables S3,4 & 6 are missing or wrongly assigned -> Supplementary tables are a mess
- Line 163 & 166: please define what control cells represent (cells with SMN1 basal mRNA levels? Or just the same cells – DMSO influence – as mentioned in line 194?) -> for immunohistochemistry it is mentioned what control is as cells – not for drug testing (line 433) and for Figure 5 (line 640)
- Fig 5d: CSP are significantly different between DMSO and PK4C9, however, they have the same

direction, indicating the same underlying structural change (potentially in this case destabilization)? – please explain -> U11 different trend
- Fig 6g: U19 data missing, hence line 273 not possible to observe (U19 also missing in 6C)
- Please make an overview table over mutants and effects (E7 inclusion, terminal opening, tri/penta-loop distribution, PK4C9 activity, stability)
- Line 148 TSL-2 interacting
- Line 376 "one of the few examples ..."
- Suppl. line 280, comparisson (with just one s)

Reviewer #4:
Remarks to the Author:
Garcia-Lopez et al describe the identification of a novel small molecule binder of the TSL2, RNA stem loop structure in the SMN2 gene. Using a combination of NMR, Next generation sequencing and mutagenesis studies they go on to show that PK4C9 binds to TSL2, promoting a conformational shift that favors increased inclusion of SMN2 exon 7.

The current study represents the first study describing the identification of a small molecule modulator of TSL2 but the importance of TSL2 as a key element in regulating SMN2 splicing has been previously well documented (Singh et al; NAR, 2007) and is recognized as an attractive target in the field.Additionally, the idea of using small molecules to target RNA secondary structure has attracted a lot of attention and has clear precedent (e.g Velagapudi et al; NCB 2013; Childs-Disney et al; ACS Chem Biol 2014; Velagapudi et al; PNAS, 2016; Patwardhan et al, MedChemComm 2017). Hence, the current study does not offer any significant advancement in our understanding of achieving SMN2 splicing modulation.

1. While the authors performed a screen for TSL2 interactors and identified their top hit PK4C9 using this approach, they fail to provide any compelling evidence for the selectivity of their hits. It is critical that they counter-screen their hits on unrelated, control RNA secondary structures to provide evidence that PK4C9 and related hits do not act as promiscuous RNA binders.

2. The binding activity is only demonstrated indirectly using fluorescent techniques, well-known to be prone to false positives, without any counter-screen data. The structural aspect of compound binding is simulated based on RNA NMR data, virtual docking and molecular dynamics. While the authors do show NMR shifts of RNA when compounds are added, these could well be conformational changes in RNA which could be induced by metal ion contaminations in the compound or by metal ion chelation by the compound (the compound does resemble a chelator). Can they rule out this possibility? Can they show shifts in compound spectra as well? Bottom line is that they show no evidence for direct, selective binding such as SPR and ITC. It is imperative that they provide direct evidence of compound binding to TSL2 using independent, label-free biophysical methods as suggested above. They should also provide an assessment of binding selectivity using control RNA structures when carrying out these assessments.

3. Do the authors have any evidence for dose responsiveness of their compound in the SMN2 mini-gene or SMN protein assays? The effect in the minigene assay and in the SMA patient fibroblast splicing assessment (Fig 3) looks like an all or none response. The protein increase in Fig 4a is very modest at the single dose (40uM) for which data is shown. In the minigene assay (Fig 3 a) it looks like PK4C9 and BJGF466 elicit maximal exon 7 inclusion at early timepoints and the effect tends to get weaker at the 24 hr time-point. Do the authors have an explanation for this? Have they looked at later time points?

4. A time course (up to 72 hrs or longer) study in dose response format is needed to make a confident statement about the cytotoxicity of these molecules. A 24 hr cytotoxicity study as shown

in Fig 3d is inadequate and a tad misleading although it shows PK4C9 to be superior to the other tested molecules at one early timepoint and at a given dose. Given that there are over 200 splicing events impacted by the molecule a more thorough evaluation of cytotoxicity is warranted.

5. In their RNA-Seq experiment the authors identified 290 transcripts with modified splicing relative to DMSO. The scope of alternative splicing events impacted by the compound may be an underestimate given that sequencing reads could not unambiguously mapped on to full length transcripts . A more stringent statistical assessment of the splicing changes and a rank ordering of the changes based on significance would be very informative. Also, It would be good for the authors to clarify which of the splicing events are due to rescue of SMN2 splicing and which may be resulting from non-specific interactions of the compound with other RNA sequences or RNA secondary structures, genome wide. Comparison of the RNA Seq profile of PK4C9 in wild type versus SMA patient fibroblasts could offer insights on this front. Alternatively, comparison to SMN overexpression / rescue or to Spinraza treatment would be informative in this regard.

6. The authors should seriously consider including a structurally related, inactive (in SMN assays) compound as a negative control in their key cellular and biophysical studies, NGS etc

7. In recent years there has been significant progress in identifying small molecule and antisense-oligonucleotide based approaches to enhancing SMN2 splicing / exon 7 inclusion. Almost all of these approaches have relied on a couple of mouse models of SMA to demonstrate in vivo efficacy. The current study however provides evidence of in vivo efficacy in a less commonly used fly model of SMA. This does not allow for proper benchmarking / comparison of TSL2 modulators to previously demonstrated approaches to enhancing SMN2 exon7 splicing that are currently in the clinic, which is critical given the current state of the field.

While Garcia-Lopez et al present promising, early evidence for the identification of small molecule modulators of the TSL2 stem loop structure in SMN2 the study fails to provide thorough validation and selectivity assessment of the compound(s). The current study represents a modest, incremental increase in our structural and mechanistic understanding of how TSL2 (which has long been known to be a key regulatory region for SMN2 splicing) may be modulated with small molecules to enhance SMN2 exon 7 inclusion.

In summary, I would not recommend accepting this manuscript for publication in its current form.

Reviewer #1

We thank the reviewer for their time and constructive comments. We have performed additional experiments and text modifications to address their concerns, as detailed below. To aid reading of the revised manuscript, all major changes have been highlighted in yellow.

Remarks to the Author:

The manuscript of Garcia Lopez et al describes the identification of a small molecule (PK4C9) as a modulator of SMN exon 7 splicing through its interaction with the TSL2 RNA loop located on the 5'ss of exon 7. The data is well described and the authors present a thorough study of the mechanism of action of PK4C9.

Specific comments are as follows:

1- In Fig 1b the visual estimation of the intensity of the western bands not always match with the scanning data presented in Fig 1c. In particular for the mutant TSL2 4G (5th lane). In fact, while in the western I would guess is even less E7 inclusion that in the SMN 2 TSL2nm (second lane) in the scanning appears slightly higher. An inconsistency between western and scan may also be present with the mutant 9C.

First, we would like to clarify that that Fig. 1b represents RT-PCR products resolved by agarose gel electrophoresis, not Western Blot lanes as indicated by the reviewer. We acknowledge that this was not immediately clear and have clarified it in the figure legend. Regarding the visual inconsistency between Fig. 1b and 1c, we now **show more representative images** of our results in **Fig 1b**. In addition, we have **re-quantified** all of our gel images with a second software (www.gelanalyzer.com), which confirmed the findings initially plotted in Fig. 1c.

	IMAGE J			GELANALYZER		
	AVG	SE	N	AVG	SE	N
SMN1 n.m.	89.9	0.6	5	100.0	0.0	5
SMN2 n.m.	16.7	2.8	8	17.3	3.8	8
SMN2 2C	10.9	1.0	8	0.0	0.0	8
SMN2 3C	54.7	5.2	8	58.9	7.6	8
SMN2 4G	21.5	1.5	8	24.8	1.7	8
SMN2 6C	62.6	4.5	8	60.8	4.3	8
SMN2 9C	47.6	6.7	8	50.1	4.9	8

27 **2- In Fig 1e the meaning of "others" should be explained in the figure legend**

28 RNA sequences that fold into hairpins possess the intrinsic potential to form duplexes
29 given their self-complementarity. In Fig. 1e, RNA samples were folded by snap cooling,
30 which favors hairpin formation over duplex interactions. Using non-denaturing PAGE we
31 could confirm the presence of the TSL2 hairpin (lower band) together with a second
32 conformation (upper band; previously named as "other"), which is consistent with the
33 presence of duplexes, based on the following:

34 (1) comparison with the expected band size of the RNA ladder. The **ladder** has now
35 been included in **Fig. 1e** for clarity.

36 (2) denaturing electrophoresis conditions using Urea (see **new Supp. Fig. S2**) confirmed
37 that the two bands observed under native conditions represent folding states, and not
38 contaminants from the RNA synthesis.

39 (3) TSL2 duplexes could be observed by NMR under experimental conditions known to
40 favor duplex formation, including high RNA concentration, high salt content, or high
41 temperature[1] (not shown). When increasing RNA and salt concentrations, the upper
42 band from our native gels also increased (see **new Supp. Fig. S2**).

43 We have modified Fig. 1e and its legend to include this information, as well as generated
44 the **new Supp. Fig. S2**.

45

46 **3- Page 5 lines 112-114 The authors interpret the effect of the 4G mutation in**
47 **structural terms, they should discuss also the possibility of creating a splicing**
48 **factor binding site that in turn inhibits splicing of exon 7 independently of the**
49 **structure. The 4G mutation seems to expose a sequence GUAAGGAGU that**
50 **although not fully "canonical" could be a binding site of hnRNPA1 or other**
51 **proteins of that family whose binding will in turn hamper 5'ss recognition**

52 In a previous report[2], nearly no increase in *SMN2* E7 splicing was observed upon
53 mutating residue 16G, which is the base pair of 4C. This supports a conformational
54 interpretation on the low splicing impact of modifying this region of the hairpin, rather
55 than a primary sequence effect by mutation 4G. Moreover, the canonical binding
56 sequence of hnRNPA1 has been well defined as UAGGGA/U[3], which differs slightly from
57 the sequence generated by the 4G mutation. However, we agree with the reviewer in

58 that we cannot completely rule out that mutation 4G triggers binding of hnRNPA1 or
59 other inhibitory splicing factors. We have, therefore, incorporated this consideration into
60 the manuscript:

61 *"The 4G mutation triggered the strongest conformational changes in TSL2. However,*
62 *SMN2 splicing was only mildly affected, suggesting that a certain level of TSL2 structure*
63 *is required for exon inclusion, or that the binding sequence of a splicing factor may have*
64 *been affected by this mutation."*

65

66 **4- Minor point, there is a typo in Page 7 line 148 TSL2-interacting**

67 This typo has now been corrected.

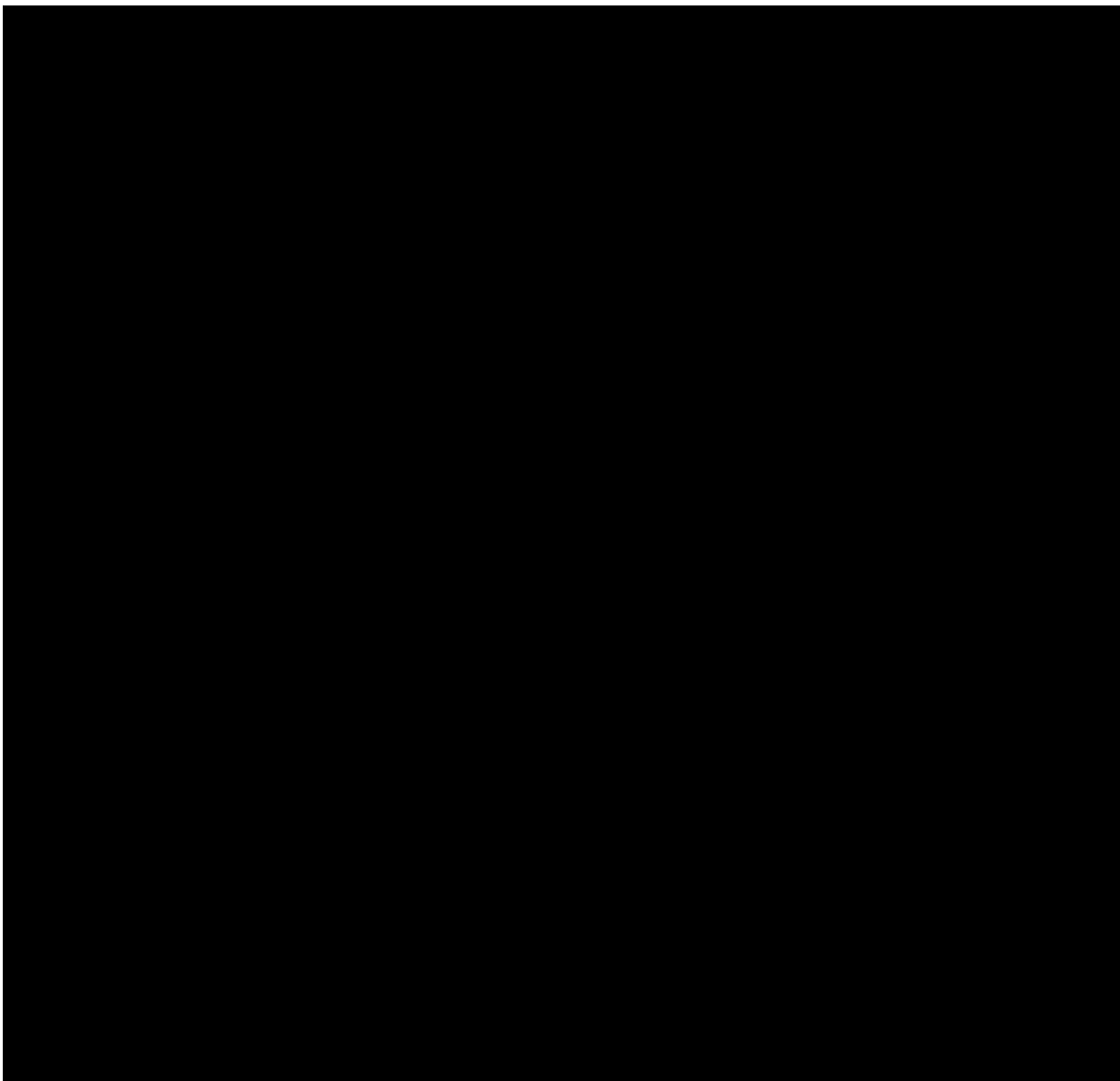**6- Fig 4a and Page8 lines 182-187: It is surprising that with the almost total restoration of normal exon 7 inclusion at the RNA level (Fig 3b and 3c) there is such a marginal increase in protein as seen by western blot. The recovery of the gems (Fig 4b) is certainly impressive but a measure of the total amount of mRNA containing exon 7 before and after treatment with PK4C9 is worth doing. The qPCR tends to give overestimates of the functional intact mRNA present in the cell, a Northern blot will give a more definitive result of the mRNAs including and excluding exon 7.**

We completely understand that a 1.5-fold increase in SMN protein levels (Western blot) might seem insufficient compared to the total correction of *SMN2* E7 splicing. However,

107   this is quite commonly seen in the SMA literature. To the best of our knowledge, more
108   than a 2-fold increase in SMN protein has not been reported for a small molecule
109   modifier of *SMN2* splicing, unless such molecule also increases *SMN2* expression levels
110   by activating transcription (*f.e.*, Valproic Acid, VPA[4]; see **Table below**). This can be
111   explained because the amount of protein that a splicing modifier can induce is limited by
112   the number of *SMN2* mRNA copies present in the cell. A 2-fold increase in SMN protein,
113   however, has been shown to (1) be sufficient to reverse SMA phenotypes in mice
114   models, including life span and motor function[9], (2) be the difference between the
115   GM03813C fibroblast line (SMA type I, the most severe type of SMA) and the
116   GM03814B line (a phenotypically unaffected individual) (see Fig. 4a of our study), (3) is
117   the value range of some of the small molecules that have recently reached clinical trials
118   for SMA (f.e., trials NCT02268552 and NCT03032172).

Examples of small molecules known to change *SMN2* E7 splicing and SMN protein levels				
Molecule	E7 splicing fold (PCR)	Protein fold (WB)	Increases *SMN2* transcription?	Reference
PK4C9	1.9 (semi-quantitative PCR) 3.0 (qPCR)	1.5	No	(our study)
C1	1.9	1.7	No	9
C2	1.9	1.5	No	9
C3	1.7	1.5	No	9
NVS-SM1	~15	1.6	No	10
NVS-SM2	~2	1.6	No	10
Hydroxyurea	≤3	≤1.94	No	11
VPA	1.8–5.2	1.8-4.2	Yes	4

119   qRT-PCR has been used as the gold standard to evaluate *SMN2* E7 inclusion, and the
120   primers and Taqman probe used in our study have been validated by us and others[9].
121   qPCR has higher sensitivity and reliability over a greater dynamic range of RNA
122   concentrations than other techniques, including semi-quantitative PCR or Northern blot.
123   In fact, we have found in the past that *SMN2* expression levels are too low to be
124   detected by conventional Northern blot protocols, unless enhanced detection with
125   radioactivity is used (to which we do not have access).

126   Based on all this, we hope that the reviewer will agree with us that a Northern blot would
127   bring little added value to the manuscript.

128

129   **7- It is not clear how the authors differentiate PK4C9 effects on splicing due to**
130   **SMN recovery or to a direct off target effect of PK4C9. The eventual off target**
131   **effects seen in WT fibroblasts after PK4C9 treatment should be more widely**

132 **discussed particularly on the light of potential use as a therapeutic agent.**

133 Our RNA sequencing (RNA-seq) analysis detected 201 differentially spliced genes with

134 an absolute PSI (percent spliced in) >0.4 upon treatment of human SMA fibroblasts

135 (GM03813C) with PK4C9 (40 μM, 24 h). A series of studies in mice have previously

136 shown that reduction of SMN protein results in widespread splicing abnormalities, the

137 identity of which depends on the genetic model, experimental conditions, and tissue/cell

138 lines used. For example, the following numbers of dysregulated splicing events have

139 been reported in SMN-depleted mice cells: 145 (motor neurons)[12]; 252 (spinal cord,

140 post-symptomatic stage), 16 (spinal cord, pre-symptomatic stage)[13]; 104 (motor

141 neurons), 86 (white matter)[14]; 259 (spinal cord), 73 (brain), and 633 (kidney)[15]. It is

142 therefore not surprising that the recovery of SMN protein induced by PK4C9 in SMA

143 fibroblasts is coupled with a large number of splicing changes, which could represent the

144 reversal of at least part of such generalized splicing abnormalities and be of therapeutic

145 relevance. ~25% of the changes found in our RNAseq study affect genes altered in

146 previous reports in mice. However, a formal comparison between ours and these

147 previous results has not been conducted in our study, given that the identity of specific

148 exons and introns affected in SMN-depleted mouse nerve cells has been shown to not

149 translate to human SMA fibroblasts[12].

150 Besides PK4C9, there are only two other examples of *SMN2*-splicing modifying small

151 molecules in the literature for which RNA-seq data also exist, the chemical scaffolds of

152 which differ notably from PK4C9. In particular:

153 (1) Novartis: NVS-SM1 (100 nM). 35 differentially spliced genes with PSI>0.4 were

154 identified[10].

155 (2) Hoffmann-La Roche: SMN-C3 (500 nM). 13 differentially spliced genes with PSI>0.4

156 were identified[9].

157 In these two cases, the molecules tested were not direct hits from a chemical screen

158 (like PK4C9), but chemically optimized leads with maximized cellular potency (nM range)

159 and oral availability. A fair comparison of these two molecules with PK4C9 can therefore

160 not be made, since PK4C9 is still in the pre-optimization stage. However, we did find

161 three differentially spliced genes (*SMN2*, *SLC25A17*, and *VPS29*) in common between

162 the three studies (see **Venn Diagram** below), further supporting that at least some of all

163   PK4C9-induced splicing changes represent a positive consequence of SMN protein

164   rescue.
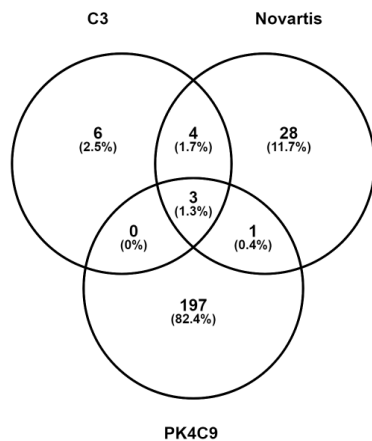
Venn diagram. Genes where alternative splicing events were detected with an absolute PSI of at least 0.4 between treated and control samples. There are three genes that were affected by all three compounds. http://bioinfogp.cnb.csic.es/tools/venny/index.html. We would be happy to include this figure in the manuscript should the reviewer agree.

165   However, part of the PK4C9-sensitive splicing changes are also likely to be off-targets.

166   In this regard, it is important to keep in mind that PK4C9, in its current state, is not

167   intended as a therapeutic agent, but as a proof-of-concept molecule that will undergo

168   chemical optimization to become a more potent and specific lead compound. Being able

169   to discern between undesired PK4C9-induced off-target *vs.* SMN recovery-mediated

170   splicing changes is key for the chemical optimization of PK4C9's specificity. In an initial

171   low-scale attempt, we compared the effect of PK4C9 on eight of these genes in SMA *vs.*

172   WT fibroblasts. To do this, we assumed that (1) true off-targets would be similarly

173   affected by PK4C9 in WT and SMA cells, but that (2) SMN-dependent changes would

174   respond differently to treatment in WT *vs.* SMA cells, given their different SMN starting

175   levels (see Fig. 4d). Four out of these eight genes belonged to the first case and the

176   remaining four to the second, confirming the co-existence of both effects. We now plan

177   to expand this analysis to the rest of transcripts and to combine this information with our

178   structural results (see Fig. 5, Fig. 6 and Fig. 7), in order to lead the optimization of

179   PK4C9's specificity.

180   Finally, a number of less-active, **structural analogues of PK4C9** that do not affect

181   *SMN2* E7 inclusion, and which were synthesized for the revised version of this

182   manuscript (see **new Supp. Fig. S8**), also failed to modify the splicing of two of the

183   transcripts that we classified as SMN-recovery dependent, further validating our

184   conclusions.

185   **Mentions to all these points** have now been added to the Results and Discussion

186   sections of the revised version of our manuscript.

Reviewer #2

We thank the reviewer for their time and constructive comments. We have performed
additional experiments and text modifications to address their concerns, as detailed
below. To aid reading of the revised manuscript, all major changes have been
highlighted in yellow.

Remarks to the Author:

In this manuscript Garcia-Lopez et al. identified a natural compound binding to the stem-
loop RNA structure of SMN2 exon 7 and report a detailed characterization of the mode
of action of this compound in vitro, in cells, and in drosophila. The manuscript contains a
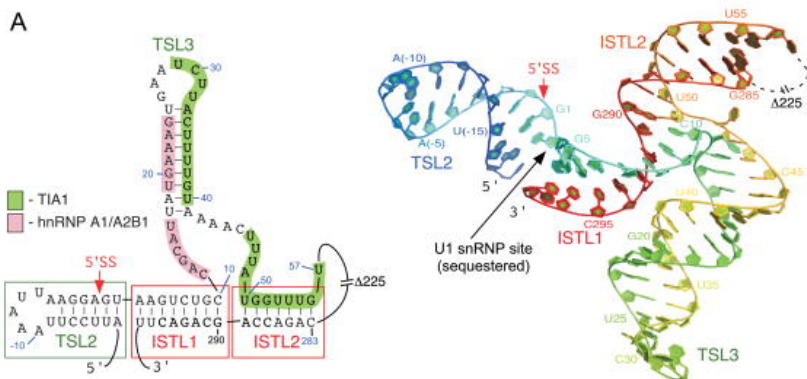large amount of data, is technically sound, and a piece of work of high quality.

However, there are several points that need to be addressed before the manuscript is
suitable for publication.

1. This regards in particular the fact that the compound binds to the terminal ends
of the stem loop structure. In the in vivo situation the terminal ends are not freely
available. Is the interaction mode determined by NMR and MD compatible with this
in vivo situation?

To the best of our knowledge, the only techniques that allow for probing of RNA
structure *in vivo* include the recently developed FragSeq, SHAPE-Map, DMS-MaPseq,
and their variants. All these methods are based on enzymatic (FragSeq[16]) or chemical
(SHAPE[17], DMS[18]) modification in living cells of RNA residues when these are in a single
strand environment, coupled to deep sequencing to detect such modifications.
Unfortunately, these are complex techniques currently used by only a few laboratories,
and that are beyond the expertise of the authors of this manuscript.

The *in vitro* version of SHAPE, however, has been previously performed on a synthetic
RNA with the SMN2 E7/I7 junction sequence[19]. The proposed secondary structure of
TSL2 from this study is consistent with our NMR and MD findings (see Figure below).

Model of the structure of the 5' ss of *SMN2* E7. Secondary structure probed by SHAPE (left). Predicted 3D structure model (right). The 3D structure is modeled on chemical structure probing and not defined by experimental constraints

216   Finally, to further address the concern of the reviewer, we have used NMR to investigate

217   an **extended version of TSL2** (TSL2 23mer) that better mimics its *in vivo* context. In

218   particular, the TSL2 23mer contains the sequence of TSL2 (TSL2 19mer) flanked by two

219   residues on each side from the endogenous *SMN2* sequence (5'-AC-19mer-AA-3'). The

220   23mer sequence forms essentially the same hairpin as the 19mer, as visible by

221   comparison of the respective **1D spectra** (see Figure below); and so are the interactions

222   with PK4C9, as measured by **WaterLOGSY** spectra (see Figure for point 5 of this

223   reviewer, page 13).
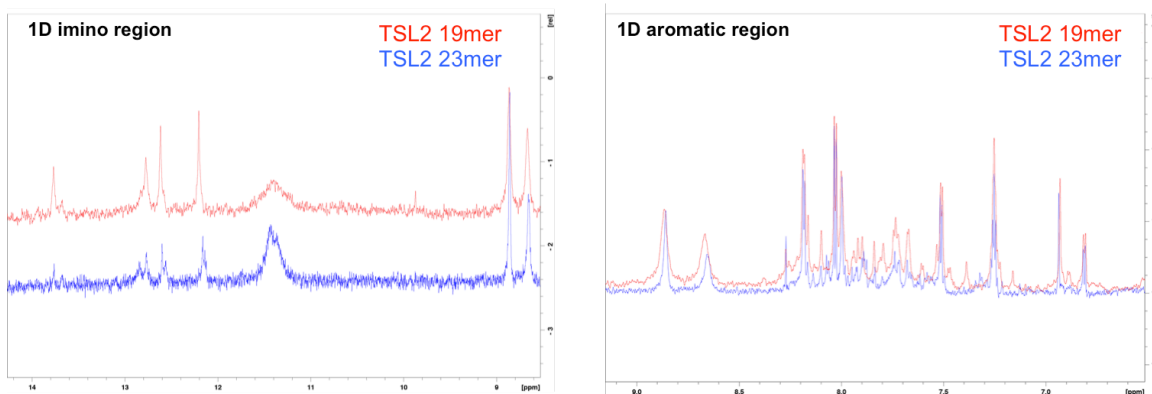
224   **TSL2 19mer *vs.* 23mer**. The 1D spectra of TSL2 19mer and TSL2 23mer show that the RNA

225   hairpin is being formed in both cases. Figures show 1D proton spectra of the imino and the

226   aromatic resonance region. For the aromatic resonances, the excitation sculpting scheme was

227   employed to suppress the water resonance and for the iminos, the jump-return echo sequence was

228   employed. We would be happy to include this figure in the manuscript should the reviewer agree.

229

230   **2. From figure 6 d and 6 there seem to be only a few contacts between the natural**

231 **compound and the RNA. Wouldn't the authors expect a broad range of unspecific**

232 **effects?**

233 We understand the concern of the reviewer. However, there are a number of examples

234 of small molecules that interact selectively with RNA through a low number of hydrogen

235 bond contacts combined with a significant hydrophobic contribution. For example, the

236 small molecule inhibitor of viral replication DB213 bound to the HIV-1 frameshift site

237 RNA (PDB code: 2L94); the RBT550 inhibitor of the HIV-1 TAR RNA, where the indole

238 moiety interacts with its target exclusively via hydrophobic contacts and π-π stacking

239 (PDB code: 1UTS); or natural product Theophylline, which also binds to an aptamer

240 RNA through hydrophobic and π-π stacking interactions (PDB code: 1O15).

241 Aminoglycosides, a class of antibiotics, also bind to ribosomal RNA only via electrostatic

242 interactions[20]. In our previous version of the manuscript, 40-ns MD simulations identified

243 a few but significant hydrogen bond contacts between PK4C9 and TSL2 residues U2

244 and U19, as well as π-π stacking with G18 and hydrophobic interactions with A1 and

245 U3. In our revised version, this **analysis has been extended** to 100 ns, in order to

246 increase the statistical significance of our findings. The extended simulations

247 corroborated the combined contribution of hydrogen bonds, π-π stacking, and

248 hydrophobic contacts to the binding mode of PK4C9 (see representative conformations

249 in the figure below and revised **Fig. 6**). To allow for a more detailed visualization of these

250 interactions, two Supplementary Videos (**Supp. Vid. V1** and **Supp. Vid. V2**) from our

251 MD simulations have been included to the revised manuscript.

a, 40 ns
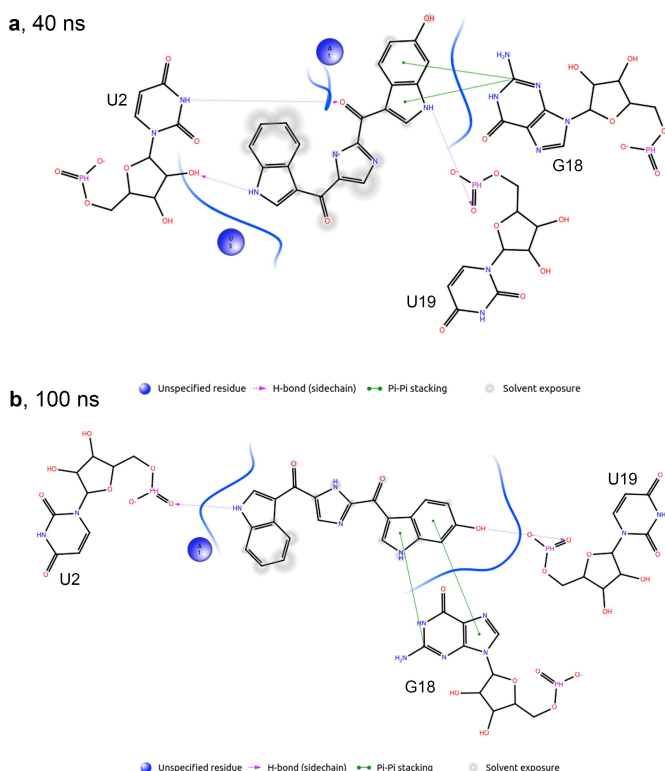
b, 100 ns

2D view of the interaction between TSL2 and PK4C9. Representative structures from the most populated clusters of the 40-ns (top) and extended (100-ns, bottom) MD trajectories. Similar interactions were found for both trajectory lengths. Interactions were plotted using the Maestro software. Note that these images show static snapshots structures. Slight dynamic changes in the interactions can occur during the trajectory.

252   We do, however, acknowledge the presence of non-specific, off-target effects of PK4C9,

253   as already discussed and observed in our RNA-seq experiment. This aspect will be

254   addressed during the chemical optimization phase of PK4C9 to convert this hit molecule

255   into a more potent and specific lead compound, taking advantage of our acquired

256   understanding on how PK4C9 interacts with its target.

257   A **more detailed discussion** of these considerations has been included in the revised

258   version of the manuscript.

259

260   **3. The NMR chemical shift perturbations shown in Figure 5d seem rather small to**

261   **me given that the compound has aromatic rings. Wouldn't the authors expect**

262   **larger chemical shift perturbations due to ring current effects.**

263   Ring current effects or binding effects would be best observed on the U2 imino proton

264   and the G18 imino proton. Unfortunately, G18 and U2 imino protons are generally

265   invisible by NMR due to fast water exchange and are therefore poor reporters. In

266   addition, when adding PK4C9 to the RNA the presence of DMSO does not allow for

267   reducing temperature, which would reduce exchange.

268

269   **4. Do the chemical shifts back-calculated from the MD model match what they see**

270   **in the spectrum?**

271   Chemical shift prediction based on our MD models was not attempted due to two main

272   reasons. (1) Whilst a plethora of empirical structure-based chemical shift predictors have

273   been developed for proteins[21-26], unfortunately only a few such methods exist for RNA

274   (f.e., NUCHEMICS[27] or SHIFTS[28]). These programs can predict nonexchangeable ^{1}H

275   chemical shifts, but are generally not precise enough for imino protons. (2) The relatively

276   short time scale of our MD simulations (100 ns) is not sufficient for reliable back-

277   calculation of certain parameters that have been reported to require simulation times >1

278   μs (f.e., J-couplings across hydrogen bonds)[29]. However, a number of observations

279   cross-validate our NMR and MD structural results. For example, (1) both NMR and MD

280   identified the same TSL2 residues (*i.e*, U2 and U19) as mediators of PK4C9 binding; (2)

281   NMR and MD found a similar proportion of triloop and pentaloop conformations in the

282   TSL2 ensemble; and (3) our combination of NMR and MD lead to predictions on the

283   effect on E7 splicing of the 2A, 2C, 3G17C and 8G12C TSL2 mutations that could be

284 validated experimentally in human cells (see Fig. 7).

285 We have now **revised the text** of our manuscript to include clarifications to the points 3
286 and 4 of the reviewer.

287

288 **5. Did the authors follow the chemical shift changes of the ligand by NMR and**
289 **could they validate their MD data with respect to the ligand - stem-loop RNA**
290 **interactions shown in Figure 5?**

291 PK4C9 showed very small CSPs upon titration with RNA excess, which are uniform (see
292 Figure below). To better observe weak interactions, we performed **WaterLOGSY**
293 (Water-Ligand Observed via Gradient SpectroscopY) experiments, a method commonly
294 used for primary NMR screening in the identification of compounds binding to the target
295 of interest in the μM range[30]. These experiments showed negative NOEs (*i. e.*,
296 magnetization transferred from "bound water") for the ligand in the presence of TSL2
297 19mer and 23mer, thus confirming binding of PK4C9 to TSL2 also from the ligand's side.
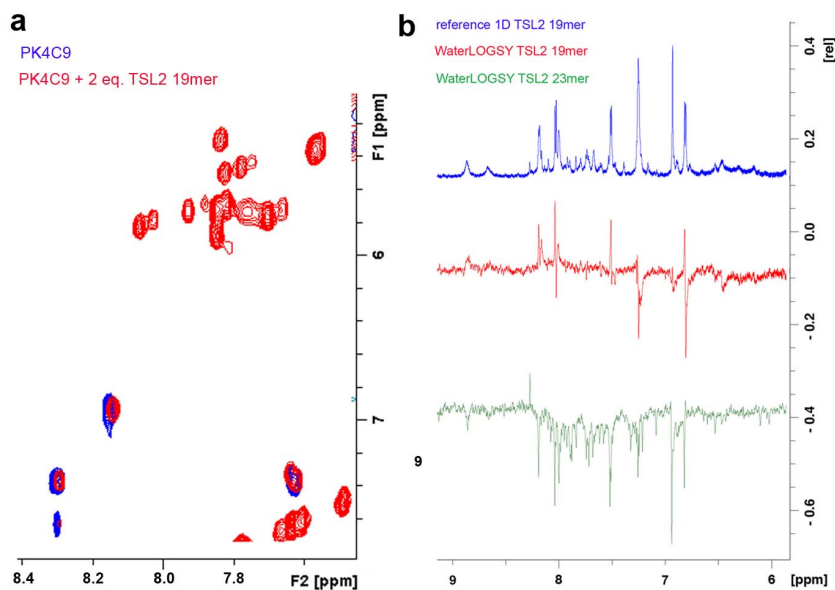
298 **PK4C9 binding to TSL2.** (a) Spectrum showing CSPs on PK4C9 upon addition of 2 equivalents of TSL2. The small
299 CSP size is likely due to low biding affinity. To overcome this, WaterLOGSY was conducted (b), which detected
300 negative NOEs, thus confirming binding. Blue: 1D reference spectrum of TSL2 plus 10-fold excess PK4C9 in 80%
301 NMR buffer, 20% DMSO-d6; red: WaterLOGSY of PK4C9 with TSL2 19mer; green: WaterLOGSY of PK4C9 with TSL2
302 23mer. We would be happy to include this figure in the manuscript should the reviewer agree.

303   **6. Minor points:** These errors have now been corrected.

304   **- some figure labels are too small and hard to read, e.g. Fig. 1a numbering of**
305   **nucleotides etc.**

306   **- some figures miss proper axes labels/units, e.g. Figure 1d (what is 'max'), Figure**
307   **1f (CD)**

308   In this particular case, we would like to note that Mol CD (Molecular Circular Dichroism)
309   are standard Circular Dichroism units.

310   **- in some figures a broken axis is shown, but there are no data points extending to**
311   **these values (e.g. Fig. 1e, Fig. 1d)**

312   **- some figures miss error bars, e.g. Fig. 1d,**

313   In this particular case, we would like to note that the standard error bars in Fig. 1d and
314   1e have been plotted, but they are too small to be visible.

315   **- Figure 3e 'Drosophila MN' is there anything missing?**

316   **- Figure 4 seems of poor resolution**

317   **Reviewer #3**

318   We thank the reviewer for their time and constructive comments. We have performed
319   additional experiments and text modifications to address their concerns, as detailed
320   below. To aid reading of the revised manuscript, all major changes have been
321   highlighted in yellow.

322

323   **Remarks to the Author:**

324   Garcia-Lopez et al show that one can use drugs (PK4C9 as most efficient) to rescue the
325   reduction of SMN1 by mis-splicing, causing SMA, by induction of a secondary structure
326   change of the isoform SMN2 becoming splicing competent at the required point. In this
327   paper many methods are coherently represented and a comprehensive evidence based
328   conclusion is drawn.

329   Most methods are standard in the field, as is most of the application. However, the
330   detailed structural work for finding out the mechanism of drug action is unusual and
331   brings out new information about this drug and the splicing mechanism - at least partial -
332   some of this was already suggested at lower resolution. This work is well done and
333   should set a standard for the field of drug development on RNA drugs - to include more
334   detailed mechanistic studies with the completeness of methods.

335

336   **Major points should be clarified**:

337   **1a. Line 275-277: Why is this coupling assumed? (loop formation to terminal**
338   **opening)**

339   We apologize for not having explained this conclusion more clearly. The coupling
340   between loop closing and terminal opening - which one could envision as a clothes peg,
341   where tightening from one end makes the other end open - is assumed given that the
342   distance between residues A1-U19 increases in the presence of PK4C9, whereas the
343   distance between residues A8-U12 (closing pair of the loop) decreases, even though the
344   ligand does not directly bind to this region. This is generally observed in the induced fit
345   model for ligand recognition, by which ligands may induce a conformational change in
346   the target rather than selecting a conformation from a pre-existing population.

347   **1b. …how is this interaction/conformational change information transported over**

348 **that long distance?**

349 By inducing a terminal opening of the TSL2 stem the overall structure of the hairpin has

350 to readjust in order to stay energetically stable. Tightening of the loop would be a way of

351 achieving this, as it would increase the energy levels in that region, and compensate for

352 the energy release at the other end of the hairpin. Similar phenomena have been

353 previously described, including the example of adenylate kinase[31], where upon substrate

354 binding, the enzyme increases its chain mobility in a region remote from the active

355 center. This region 'solidifies' again upon substrate release, serving as a 'counterweight'

356 balancing the substrate binding energy. A **reference to this example** has now been

357 included in the manuscript text.

358

359 **2. Could some of it simply be explained by less overall stability (e.g. U2A**

360 **mutation) -> add melting temperatures (e.g. from Fig S2, but preferred by UV),**

361 We agree with the reviewer in that TSL2 mutations and PK4C9 most likely affect the

362 overall stability of the RNA. However, simply reducing TSL2 stability in a "blind" way

363 would not necessarily aid 5' ss recognition. For example, mutation 8G12C, which has

364 the highest **melting temperature** (Tm; calculated using differential scanning fluorimetry,

365 DSF) amongst all thirteen TSL2 mutations studied (see Table & Figure below and **new**

366 **Supp. Table S1**), showed the best *SMN2* E7 inclusion values in HeLa cells transfected

367 with mutated minigenes. In fact, we did not find a significant correlation between the Tm

368 of the thirteen mutant RNAs and their impact on *SMN2* E7 splicing (see Figure below),

369 further arguing against a general stability effect on TSL2 as the reason for E7 inclusion.

370 Instead, the different mutations would trigger conformational rearrangements that may

371 directly or indirectly improve accessibility of the 5' ss. This idea is in agreement with our

372 2-amino purine (2AP), Circular Dichroism (CD), and MD results (Fig. 1 & 6, **Supp. Table**

373 **S1**), and with the fact that mutation 8G12C can increase 5' ss accessibility despite being

374 located at the other end of the stem.

375

Tm values of TSL2 mutants obtained by differential scanning fluorimetry (DSF)												
	4G	2G	9C	3C	**WT**	17C	6C	3G	3A	3G17C	2A	2C	8G12C
Tm	41.2	42.0	44.7	45.5	**45.6**	47.6	48.7	49.2	51.1	51.0	51.5	51.8	52.2
± SE	±0.16	±0.02	±0.05	±0.00	**±0.07**	±0.03	±0.09	±0.05	±0.05	±0.05	±0.07	±0.06	±0.02

376
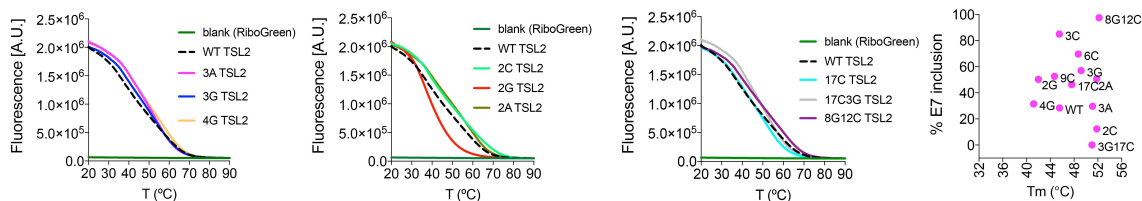
Representative DSF curves. Upon request by the reviewer Tm values were obtained by DSF, as described in[32] (n=8, Boltzmann sigmoidal fitting). A plot showing no correlation between Tm values and *SMN2* E7 inclusion is included (right)**.** UV melting curves could not be obtained due to lack of appropriate equipment. We would be happy to include this figure in the manuscript should the reviewer agree.

3. Line 129-132: would that not also decrease specificity?

The reviewer raises the concern that the screening of focused chemical libraries may decrease hit specificity. On the contrary, the use of focused libraries has increased notoriously in recent years, due to a number of benefits, as reviewed in refs.[33,34]. For example, commercially available, high-chemical diversity libraries are generally biased for modulating protein function, thus yielding much lower hit rates for RNA targets (0% to 1%, ref.[35] plus our own experience and personal communications). In addition, often the hits identified are not specific for the RNA probed and are likely to have protein off-targets[36]. In contrast, a well-designed, target-focused library with privileged scaffolds to bind RNA can (1) save time and money by reducing the number of compounds to be experimentally tested, (2) yield higher hit rates by eliminating compounds that are unlikely to bind to the target[35,37], and (3) find more potent and selective binders, as it has been shown for inhibitors of the c-Src kinase[38].

It is of course a possibility that hits from a focused library of RNA binders bind to more than one RNA target, which is a common concern to all chemical screening campaigns. Typically, these campaigns are followed by a chemical optimization phase of the identified hits into clinical candidates, where specificity is closely monitored throughout the process. In this regard, having performed a target-based screening poses a big advantage *vs.* phenotypic screening approaches, since our knowledge on the mechanism of action of PK4C9, coupled with our RNA-seq findings, will accelerate the optimization of PK4C9's specificity. It is also worth noting that focused collections often offer molecular starting-points that dramatically reduce the subsequent hit-to-lead optimization timescale, given that the properties of their compounds have already been

16

405 filtered to suit the type of target in question.

406 A **mention to focused library screening** has been added to the Discussion of the
407 revised manuscript.

408

409 **4. Some minor changes need to be addressed:**

410 **a. line 114/115: what indicates the native page conclusion of hairpin formation? –**
411 **more detail please (e.g. marker…)**

412 RNA sequences that fold into hairpins possess the intrinsic potential to form duplexes
413 given their self-complementarity. In Fig. 1e, RNA samples were folded by snap cooling,
414 which favors hairpin formation over duplex interactions. Using non-denaturing PAGE we
415 could confirm the presence of the TSL2 hairpin (lower band) together with a second
416 conformation (upper band; previously named as "other"), which is consistent with the
417 presence of duplexes, based on the following:

418 (1) comparison with the expected band size of the RNA ladder. The **ladder** has now
419 been included in **Fig. 1e** for clarity.

420 (2) denaturing electrophoresis conditions using Urea (see **new Supp. Fig. S2**) confirmed
421 that the two bands observed under native conditions represent folding states, and not
422 contaminants from the RNA synthesis.

423 (3) TSL2 duplexes could be observed by NMR under experimental conditions known to
424 favor duplex formation, including high RNA concentration, high salt content, or high
425 temperature[1] (not shown). When increasing RNA and salt concentrations, the upper
426 band from our native gels also increased (see **new Supp. Fig. S2**).

427 We have now modified Fig. 1e and its legend to include this information, as well as
428 generated the **new Supp. Fig. S2**.

429 **4b. CD experiments: melting curves: maybe the effect is caused by difference in**
430 **stability rather than conformation?**

431 Conformational and stability changes are linked – it is through conformational changes
432 that the overall thermodynamic stability of a structure is affected. In the manuscript, we
433 chose to use the expression "conformational changes" rather than "stability changes" to
434 avoid confusion. For example, a mutation can stabilize (*i.e.*, freeze) the RNA in a
435 particular conformation that makes the overall structure less stable (i.e., lower melting

17

436 temperature, Tm) - this mutation could therefore be considered as stabilizing or
437 destabilizing depending on which of the two things are being discussed. Assuming that
438 the reviewer means stability in terms of Tm, we refer to our **new Supp. Table S1**; where
439 a summary of our 2-amino purine, circular dichroism, and native PAGE results clearly
440 shows that the different mutations induce conformational changes, the magnitude of
441 which correlate with E7 inclusion but not necessarily with Tm values (see also Fig. 1).

442 **4c. Suppl. Table S1 is wrongly called Suppl. Table S2, Tables S3,4 & 6 are missing**
443 **or wrongly assigned -> Supplementary tables are a mess**

444 We apologize for not having organized the Supporting Material more clearly. Supp.
445 Tables S1, S3 & S4 (now renamed as S2, S4 & S5) are large Excel files that were
446 provided as separate files, whereas Supp. Tables S2 & S5 (now renamed as S3 & S6)
447 were part of the Supporting Material Word document. To avoid this confusion, the new
448 Supporting Material Word document now contains the list and captions of all Supp.
449 Tables and a reference to the corresponding Excel file.

450 **4d. Line 163 & 166: please define what control cells represent (cells with SMN1**
451 **basal mRNA levels? Or just the same cells – DMSO influence – as mentioned in**
452 **line 194?) -> for immunohistochemistry it is mentioned what control is as cells –**
453 **not for drug testing (line 433) and for Figure 5 (line 640)**

454 We have now clarified this as follows:

455 - Lines 163 & 166: controls cells are now called DMSO-treated cells. These are the
456 same cells as those treated with PK4C9, but treated with DMSO under otherwise the
457 same conditions.

458 - Line 433: our previous Methods description read: "*At 80 % confluence, cells were*
459 *treated for 24 h with DMSO (control) or PK4C9 (40 μM)*". This now reads: "*At 80 %*
460 *confluence, cells from the same cell line were treated for 24 h with DMSO (control) or*
461 *PK4C9 (40 μM)*"

462 - Figure 5a: our previous figure legend read: "*[…] AGGTAAG as the most enriched motif*
463 *in exons that are differentially spliced in SMA cells upon treatment with PK4C9 (40 μM,*
464 *24 h)*". This now reads "*[…] AGGTAAG as the most enriched motif in exons that are*
465 *differentially spliced in SMA cells upon treatment with PK4C9 (40 μM, 24 h) compared to*
466 *SMA cells treated with DMSO (24 h).*"

467   - Figure 5b-c, our previous figure legend read: "*Transfected cells were treated with*

468   *DMSO (0.04%, controls) or PK4C9 (40 μM) (n>3)*". This now reads: "*Transfected HeLa*

469   *cells were treated with DMSO (0.04%, controls) or PK4C9 (40 μM) (n>3)*".

470   **4e. Fig 5d: CSP are significantly different between DMSO and PK4C9, however,**

471   **they have the same direction, indicating the same underlying structural change**

472   **(potentially in this case destabilization)? – please explain -> U11 different trend**

473   We understand the reviewer's comment. However, CSPs and their direction are often

474   easy to over-interpret. A same trend could indeed mean the same kind of structural

475   change, but not necessarily. The chemical shift resonance of an atom is not only

476   affected by the local structural geometry, but also influenced by changes in the

477   environment (such as ligand binding, solvent, electro-negativity of nearby groups,

478   induced magnetic field effects, etc). It is, therefore, important to interpret these data

479   taking into consideration their context. In our case, the PK4C9-induced CSPs observed

480   by NMR match the contacts predicted by our non-biased MD protocol, and these two

481   things together also explain other experimental observations (*f.e.*, the behavior of TSL2

482   mutants, or of our PK4C9 structural analogues). Regarding U11, we have removed our

483   previous interpretation of the PK4C9-induced CSP for this residue, as we agree it is less

484   clear than the cases of U2 and U19.

485   **4f. Fig 6g: U19 data missing, hence line 273 not possible to observe (U19 also**

486   **missing in 6C)**

487   This mistake has been corrected. Graphs from Figs. 6c and 6g now include residue U19.

488   **4g. Please make an overview table over mutants and effects (E7 inclusion,**

489   **terminal opening, tri/penta-loop distribution, PK4C9 activity, stability)**

490   This is an excellent idea, which we have now incorporated to our manuscript as **Supp.**

491   **Table S1**.

492

493   The following mistakes have also been corrected:

494   **- Line 148 TSL-2 interacting**

495   **- Line 376 "one of the few examples ..."**

496   **- Suppl. line 280, comparisson (with just one s)**

Reviewer #4:

498 We thank the reviewer for their time and constructive comments. We have performed
499 additional experiments and text modifications to address their concerns, as detailed
500 below. To aid reading of the revised manuscript, all major changes have been
501 highlighted in yellow.

502

503 **Remarks to the Author:**

504 Garcia-Lopez et al describe the identification of a novel small molecule binder of the
505 TSL2, RNA stem loop structure in the SMN2 gene. Using a combination of NMR, Next
506 generation sequencing and mutagenesis studies they go on to show that PK4C9 binds
507 to TSL2, promoting a conformational shift that favors increased inclusion of SMN2 exon
508 7.

509

510 **The current study represents the first study describing the identification of a small**
511 **molecule modulator of TSL2 but the importance of TSL2 as a key element in**
512 **regulating SMN2 splicing has been previously well documented (Singh et al; NAR,**
513 **2007) and is recognized as an attractive target in the field. Additionally, the idea of**
514 **using small molecules to target RNA secondary structure has attracted a lot of**
515 **attention and has clear precedent (e.g Velagapudi et al; NCB 2013; Childs-Disney**
516 **et al; ACS Chem Biol 2014; Velagapudi et al; PNAS, 2016; Patwardhan et al,**
517 **MedChemComm 2017). Hence, the current study does not offer any significant**
518 **advancement in our understanding of achieving SMN2 splicing modulation.**

519 It is unfortunate that the reviewer finds our study of little novelty and we apologize if the
520 discrepancy arises, at least partly, due to poor explanation from our side. However, we
521 are convinced that our work contributes with new relevant aspects and tools to the SMA,
522 RNA splicing & drug discovery fields, and would like to emphasize some of the key novel
523 contributions of our study. In particular:

524 1. TSL2 was first described in 2007 by *in vitro* enzymatic probing, followed by *in vitro*
525 SHAPE in 2015[2,19], but no atomistic characterization of this structure has ever been
526 conducted. In our study, we have **solved the first atomistic structure of TSL2** using
527 NMR. This NMR structure has been submitted to the PDB and is now available to any

528   laboratory who wishes to conduct structural research on TSL2, both experimentally and
529   *in silico* (*f.e*., drug design, RNA-protein interaction modeling, etc). Thus, our work
530   provides a highly valuable tool that will make certain experimental designs possible for
531   the first time to different research communities.

532

533   2. The report from 2007 described TSL2 as a triloop, whereas the SHAPE study from
534   2015 found it in a pentaloop form. Here, we **resolve a discrepancy** and describe that
535   both species do co-exist. In fact, we provide the most extensive description of the
536   conformational dynamics of TSL2 (both wild type and mutated) to date using MD for the
537   first time, along with the first rational and atomistic explanation as to how the TSL2
538   equilibrium between pentaloop and triloop conformations could influence E7 splicing.
539   This information can certainly inspire other groups interested in the study of *SMN2*
540   splicing regulation, and/or in the study of stem-loops regulating splice site recognition.
541   As an example, see reference[39] - where terminal loop stability was predicted to affect
542   splice site recognition.

543

544   3. We have performed the **first target-based screening** of small molecules for SMA.
545   Several excellent small molecule phenotypic screening campaigns have been
546   undertaken for SMA, but these relied on splicing reporters in living cells, and very often
547   the mechanisms by which hits change splicing remained unsolved. This is not the case
548   in our study. Moreover, our target-based screening was conducted on an RNA target. As
549   the reviewer very correctly points out, ours is not the first use of small molecules to
550   target an RNA structure[36,40,41]. However, it is known that targeting RNA remains a
551   challenging field with still few precedents compared to proteins targets. Thus, our study
552   will contribute to the expansion of this field by providing an additional and novel
553   approach. For example, our study has generated all the necessary structural tools and
554   knowledge for other groups to attempt *in silico* drug design against TSL2. To the best of
555   our knowledge, *in silico* drug design has never been attempted for SMA.

556

557   4. Experimental target-based screenings and *in silico* rational drug design against RNA
558   structures have been attempted for Myotonic Dystrophy[42-44], cancer[45], the HIV TAR
559   RNA[46,47] or different miRNAs[48,49], among others. However, when this project started,

560 there were no clear precedents of bioactive small molecules targeting the RNA structure
561 of a splice site. Since then, two examples were published in 2014 of rational screenings
562 targeting the stem loop of the E10/I10 junction of *MAPT* [50,51]. This rather limited number
563 of precedents demonstrates that targeting RNA structures with small molecules to
564 modulate splicing is indeed a **promising field still in growth**, which will benefit from
565 additional examples.

566

567 5. PK4C9, our most promising hit from a proof-of-concept screening, offers a **new**
568 **chemical scaffold** in the SMA literature. We are aware that PK4C9 is not a final drug
569 candidate, but a starting point for chemical optimization. This optimization has the
570 potential of identifying an entirely new series of active compounds for SMA, which we
571 are committed to continue developing. The fact that PK4C9 is not in its final state has
572 the added potential of raising interest in the field by other groups that wish to contribute
573 to its development.

574 We have revised our manuscript text to include mentions to these points.

575

576 **1. While the authors performed a screen for TSL2 interactors and identified their**
577 **top hit PK4C9 using this approach, they fail to provide any compelling evidence**
578 **for the selectivity of their hits. It is critical that they counter-screen their hits on**
579 **unrelated, control RNA secondary structures to provide evidence that PK4C9 and**
580 **related hits do not act as promiscuous RNA binders.**

581 The reviewer raises an important point. Whilst we do not expect complete target
582 specificity at the current stage of development of PK4C9 (as already discussed and
583 observed in our RNAseq experiment), we agree with the reviewer in that it is crucial to
584 confirm that PK4C9 is not a pan-nucleic acid binder. To address this issue, we have
585 performed a **new experiment** using fluorescence displacement with RiboGreen (see
586 **new Supp. Fig. S6**), where binding of our top screening hit compounds to native TSL2
587 was compared with the following controls of binding selectivity:

588 1. An unrelated RNA structure. Here, NCI377363, PK4C9, and BJG466 showed a
589 significantly better interaction with native TSL2 than with the control structure (see figure
590 below), indicating some binding selectivity. 288D, however, showed weak binding to
591 both.

592 2. A partially denatured TSL2 (60 °C). A dramatic decrease in NCl377363, PK4C9 and
593 BJGF466 binding was observed when TSL2 was, at least partially, unfolded (Tm of
594 TSL2 under the assay conditions is 45.6 °C), indicating that these hits target TSL2
595 structure rather than its primary sequence, and that they do not efficiently bind to single-
596 strand RNA. Conversely, 288D binding was not affected.

597 Collectively, these results demonstrate that NCl377363, PK4C9 and BJGF466 are not
598 promiscuous RNA binders, whereas 288D seems to be.
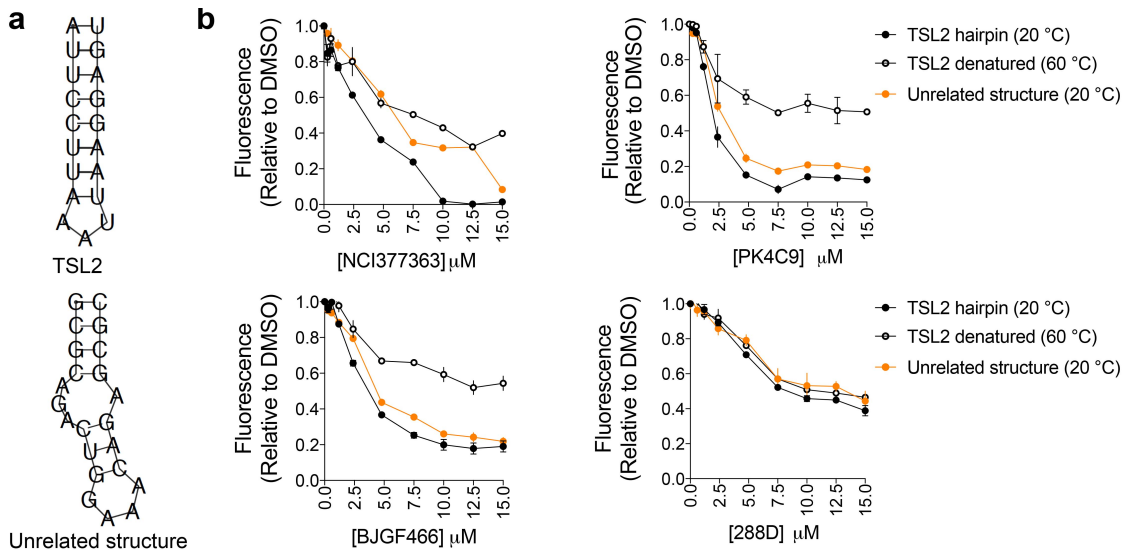
599 **NCl377363, PK4C9 and BJGF466 are not indiscriminate RNA binders.** (a) Sequence and secondary structures of
600 TSL2 and the selected unrelated RNA control (RNAfold online tool). (b) RiboGreen fluorescence displacement binding
601 assay. Upon binding of hit compounds to the RNA, the fluorescence of the dye decreases. Data points show mean
602 values ± SE (n=3). RiboGreen can bind to double stranded and to single stranded nucleic acids.

603

604 **2a. The binding activity is only demonstrated indirectly using fluorescent**
605 **techniques, well-known to be prone to false positives, without any counter-screen**
606 **data. The structural aspect of compound binding is simulated based on RNA NMR**
607 **data, virtual docking and molecular dynamics. While the authors do show NMR**
608 **shifts of RNA when compounds are added, these could well be conformational**
609 **changes in RNA which could be induced by metal ion contaminations in the**
610 **compound or by metal ion chelation by the compound (the compound does**
611 **resemble a chelator). Can they rule out this possibility?**

612 The reviewer raises two interesting possibilities:

613   1. That traces of metal ion contaminants in the synthetic sample of PK4C9 are
614   responsible for the TSL2 conformational changes observed by NMR. This possibility can
615   be safely ruled out, as the only metal ions that the PK4C9 solution contained were traces
616   from the environment, which we have quantified by **atomic absorption (ICP)** as per the
617   table below. The only metal that could have originated from the synthesis of PK4C9 is
618   palladium, which is near the limits of detection (thus truly trace amounts), and which
619   could not have affected the conformation of TSL2, as this would require a stoichiometric
620   amount of metal.

| ICP analysis of metals in the PK4C9 sample			
Element	w/w (ppm)	e(w/w)	melement (mg)
Pd	5.157370195	10.56570764	2.57869E-05
Mg	137.3612737	38.91884638	0.000686806
Fe	297.0323541	73.1320868	0.001485162
Co	0	8.820226795	0
Ni	0	9.219686127	0
Cu	0	10.68253924	0

621   2. That a potential chelating effect of PK4C9 is responsible for the conformational
622   changes in TSL2 observed by NMR. We understand the reviewer's concern due to the
623   presence of nitrogens in the composition of PK4C9. However, this concern would apply
624   to all nitrogen-containing inhibitors described in the literature. We would like to point out
625   that our NMR buffer (10 mM sodium phosphate buffer pH 6.4, 50 mM NaCl and 0.1 mM
626   EDTA) not only does not contain any metals, but it also contains the chelating agent
627   EDTA at 0.1 mM (added to protect the RNA sample from heat-induced RNase digestion
628   during RNA folding). In our ligand titration experiments, PK4C9 is used at 40-50 μM.
629   Therefore any potential chelating effect by PK4C9 would be marginal compared to
630   EDTA. Finally, even if PK4C9 acted as a transporter of metal ions from the medium into
631   the RNA, PK4C9 would have a kinetic effect only, which may be relevant in cellular
632   tests, but could not account for our *in vitro* results, as there is no kinetic barrier to metal
633   diffusion.

634   In summary, we are confident that the chemical shift perturbations (CSPs) observed in
635   our ligand titration experiments represent targeted binding of PK4C9 to TSL2. Our MD
636   simulations (performed in a metal-free simulated environment) and our NMR results are
637   convergent, and this convergence lead to predictions that could be confirmed

638 experimentally. Moreover, the same CSPs have always been obtained in every PK4C9

639 titration replicate that we have performed.

2b.Can they show shifts in compound spectra as well?

641 In TOCSY experiments, PK4C9 showed very small CSPs upon titration with RNA

642 excess, which were uniform (see Figure below, a). To better observe this type of weak

643 interactions, we performed **WaterLOGSY** (Water-Ligand Observed via Gradient

644 SpectroscopY) experiments, a method commonly used for primary NMR screening in the

645 identification of compounds binding to the target of interest in the μM range[30]. These

646 experiments showed negative NOEs (*i. e.*, magnetization transferred from "bound

647 water") for the ligand in presence of TSL2 (see Figure below, b), thus confirming binding

648 of PK4C9 to TSL2 also from the ligand's side.
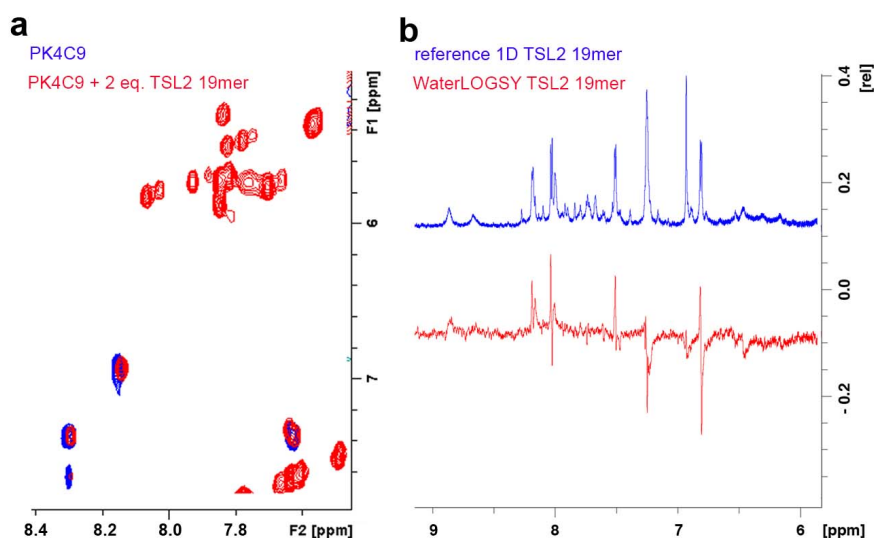
649 **PK4C9 binding to TSL2.** (a) TOCSY spectrum showing CSPs on PK4C9 upon addition of 2 equivalents of TSL2. The

650 small CSP size is likely due to low biding affinity. To overcome this, WaterLOGSY was conducted (b), which detected

651 negative NOEs, thus confirming binding. Blue: 1D reference spectrum of TSL2 plus 10-fold excess PK4C9 in 80%

652 NMR buffer, 20% DMSO-d6; red: WaterLOGSY of PK4C9 with TSL2 19mer; green: WaterLOGSY of PK4C9 with TSL2

653 23mer. We would be happy to include this figure in the manuscript should the reviewer agree

654

655 **2c. Bottom line is that they show no evidence for direct, selective binding such as**

656 **SPR and ITC. It is imperative that they provide direct evidence of compound**

657 **binding to TSL2 using independent, label-free biophysical methods as suggested**

658 **above.**

659   In our study we show proof of direct binding obtained by NMR. NMR is an extremely

660   powerful technique compared to other biophysical methods, due to its higher sensitivity

661   and atomic resolution, as well as the fact that NMR allows for monitoring of RNA integrity

662   whereas techniques like SPR or ITC do not. Nevertheless, to address the issue raised

663   by the reviewer we have undertaken additional efforts to provide further evidence of

664   direct binding. In particular:

665   1. In addition to our original fluorescent displacement (FD) assay using the TO-PRO1

666   dye, we also provide now evidence of PK4C9 binding to TSL2 using fluorescence

667   displacement with the RiboGreen dye (see Figure below). Although this is a

668   fluorescence-based technique that does not directly demonstrate binding, it rules out a

669   false positive caused by the TO-PRO1 dye.
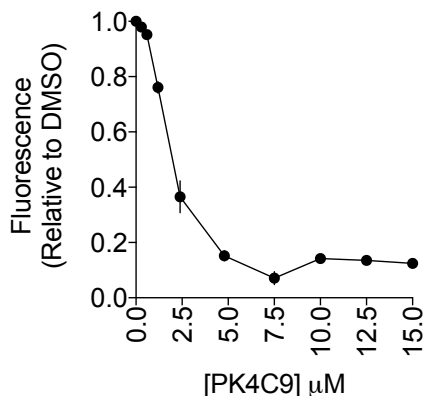
RiboGreen assay. Incubation of TSL2 with the RiboGreen nucleic acid dye in the presence of DMSO or increasing concentrations of PK4C9. When bound to TSL2, RiboGreen fluoresces. When PK4C9 binds to TSL2, the dye is released and fluorescence decreases. Signal is corrected to the blank (RiboGReen plus PK4C9 alone) and is shown normalized to the DMSO control. We would be happy to include this graph in the manuscript should the reviewer agree.

670

671   2. In collaboration with Creoptix (www.creoptix.com), we also attempted an **SPR-based**

672   **method** to detect direct binding, using the Creoptix WAVE Delta instrument instrument,

673   which measures grating-coupled interferometry signals. In these experiments, a

674   biotinylated TSL2 RNA was immobilized onto the matrix surface with PK4C9 being in the

675   mobile phase. A biotinylated DNA served as negative control. PK4C9 gave a

676   concentration-dependent signal on the tested RNA that was higher than the one

677   observed for the DNA control (see Figure below). However, we observed a residual

678   sticky effect of the ligand to the matrix surface, which although partially occurred, also to

679   a lesser extent, on an empty surface (*i.e.,* when no RNA or DNA is immobilized). Despite

680   big efforts (including trying different matrices, buffers, detergents, and controls) we could

681   not solve this technical issue, which was most likely caused by a combination of the

682   hydrophobic nature and low solubility of PK4C9 together with the need to work at high

683   ligand concentrations due to a low affinity binding, leading to precipitation of PK4C9 onto

684   the surface. Taken together, although these results showed direct binding of PK4C9 to

685   TSL2, SPR was in our case not suitable to draw a firm confirmation due to technical

686   limitations.

687
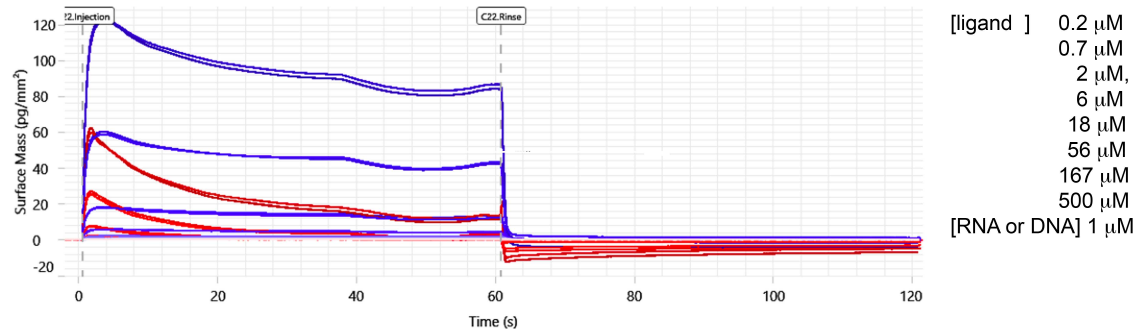
Grating-coupled interferometry signals. Surface Plasmon Resonance (SPR)-based method. Signals originated from

689   the injection of increasing amounts of PK4C9 into the captured Biotinylated TSL2 RNA (blue) or DNA (red). X axis is

690   time (s) of injection of PK4C9 from 0 to 120 s.

691

692   3. Our group has a strong expertise in **isothermal titration calorimetry (ITC)**[52,53].

693   Therefore, ITC was attempted despite some concerns with respect to the low solubility

694   and affinity of PK4C9, both of which pose important limitations to this methodology. The

695   ITC experiment showed weak binding enthalpy for an endothermic low affinity interaction

696   upon ligand titration (see Graph below). The shape of the observed binding isotherm

697   (lower panel) is reminiscent of an incompletely described binding event (c-value < 1), as

698   it would be expected for a K_D in the range of 100-200 µM. Indeed, simulating an ITC

699   titration under our experimental conditions predicted a K_D value of 100 to 250 µM for our

700   system. Unfortunately, due to the poor solubility of PK4C9 and limited availability of

701   TSL2 RNA, it is not reasonable to increase their concentrations to a level that would

702   allow measuring complex formation. Therefore, we are unfortunately limited by the

703   capacity of ITC to provide a K_D value that would firmly quantify the binding of PK4C9 to

704   TSL2.
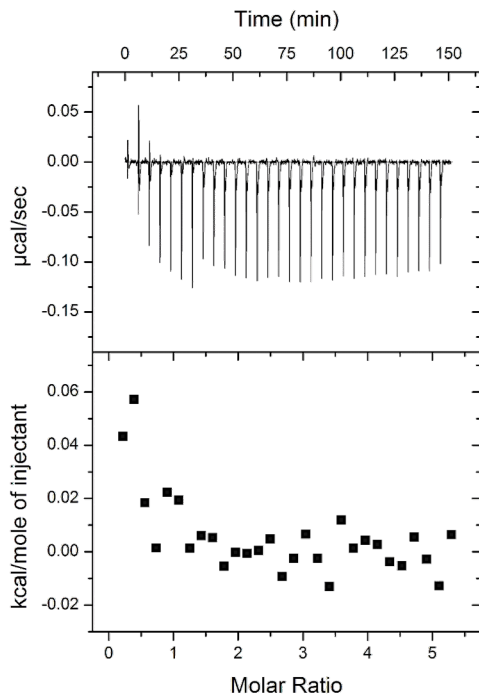
Binding of PK4C9 to TSL2 RNA measured by ITC. TSL2 (57 µM in a 1.45 ml cell) was titrated with a first 2 µl control injection followed by 29 injections of 7 µl of PK4C9 (2.0 mM in syringe) in presence of 20% DMSO. The raw data for consecutive injections of of PK4C9 to TSL2 (top panel) was integrated and corrected for the heat of dilution of the corresponding control experiment (PK4C9 into buffer; data not shown) and plotted against the [PK4C9]/[TSL2] ratio (lower panel).

705   In conclusion, we have done everything we could to address the issue raised by the
706   reviewer. Our fluorescence displacement assays, both with TO-PRO-1 and RiboGreen
707   dyes, detected binding between PK4C9 and TSL2. We could not firmly quantify the
708   strength of the binding neither by an SPR-like method nor by ITC, due to the low affinity
709   and solubility of PK4C9. However, both techniques suggest a weak but direct interaction,
710   for which no K_D could be calculated but could be estimated to be around 200 µM. NMR,
711   which has the highest resolution of all three techniques, could however detected direct
712   binding.

713   **2d. They should also provide an assessment of binding selectivity using control**
714   **RNA structures when carrying out these assessments.**

715   Please, see our answer to point 1 of this reviewer, where we conclude that PK4C9 is not
716   a promiscuous RNA binder by comparing the interaction with native TSL2 *vs.* denatured
717   TSL2 and an unrelated RNA secondary structure, using fluorescence displacement (see
718   also our **new Supp. Fig. S6**).

719   **3a. Do the authors have any evidence for dose responsiveness of their compound**
720   **in the SMN2 mini-gene or SMN protein assays? The effect in the minigene assay**
721   **and in the SMA patient fibroblast splicing assessment (Fig 3) looks like an all or**
722   **none response.**

723 As shown in Figs. 3b and 3c, the *SMN2* splicing modifier effect of PK4C9 follows a dose-
724 response curve with typical sigmoid shape, which exploits the maximum possible
725 amplitude of the response. However, we agree with the reviewer in that the
726 concentration range at which we see this dose-response (from 10 μM to 50 μM) could be
727 seen as rather narrow. This type of response may be caused by the mode of action of
728 the molecule, involving conformational changes that are thermodynamically costly, thus
729 resulting in low potency (μM range). As an example, this thermodynamic penalty has
730 been observed and characterized in the case of imatinib binding to C-Src[54]. A reference
731 to this point has now been now added to the legend of Fig. 3, which reads as follows:

732 *"The dose-response curve of PK4C9 in both cell lines reveals a rather narrow*
733 *concentration window but achieves maximal response. Concentrations higher than 50*
734 *μM could not be measured due to poor solubility of the compound under the*
735 *experimental conditions".*

736 **3b. The protein increase in Fig 4a is very modest at the single dose (40uM) for**
737 **which data is shown.**

738 We completely understand that a 1.5-fold increase in SMN protein levels (Western blot)
739 might seem insufficient, especially given the nearly total correction of *SMN2* E7 splicing.
740 However, this is quite commonly seen in the SMA literature. To the best of our
741 knowledge, more than a 2-fold increase in SMN protein has not been reported for a
742 small molecule modifier of *SMN2* splicing, unless such molecule also increases *SMN2*
743 expression levels by activating transcription (*f.e.*, Valproic Acid, VPA[4]; see Table below).
744 This can be explained because the amount of protein that a splicing modifier can induce
745 is limited by the number of *SMN2* mRNA copies present in the cell. A 2-fold increase in
746 SMN protein, however, has been shown to (1) be sufficient to reverse SMA phenotypes
747 in mice models, including life span and motor function[9], (2) be the difference between
748 the GM03813C fibroblast line (SMA type I, the most severe type of SMA) and the
749 GM03814B line (a phenotypically unaffected individual) (see Fig. 4a of our study), (3) is
750 the value range of some of the small molecules that have recently reached clinical trials
751 for SMA (f.e., trials NCT02268552 and NCT03032172).

752

753

Examples of small molecules known to change *SMN2* E7 splicing and SMN protein levels

Molecule	E7 splicing fold (PCR)	Protein fold (WB)	Increases *SMN2* transcription?	Ref.
PK4C9	1.9 (semi-quantitative PCR) 3.0 (qPCR)	1.5	No	(our study)
C1	1.9	1.7	No	9
C2	1.9	1.5	No	9
C3	1.7	1.5	No	9
NVS-SM1	~15	1.6	No	10
NVS-SM2	~2	1.6	No	10
Hydroxyurea	≤3	≤1.94	No	11
VPA	1.8–5.2	1.8-4.2	Yes	4

754 **3c. In the minigene assay (Fig 3 a) it looks like PK4C9 and BJGF466 elicit maximal**

755 **exon 7 inclusion at early timepoints and the effect tends to get weaker at the 24 hr**

756 **time-point. Do the authors have an explanation for this? Have they looked at later**

757 **time points?**

758 The effect pointed out by the reviewer was indeed observable in HeLa cells, but not in

759 fibroblasts, where the PK4C9 splicing modifier activity did increase with time (see Graph

760 below, not included in the manuscript).
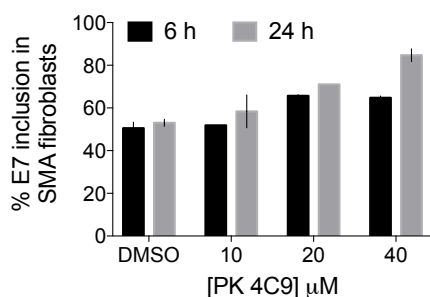
SMN2 E7 splicing upon 6h and 24 h of PK4C9 treatment. Semi-quantitative PCR results from SMA fibroblasts. Graph shows mean values ± SE (n=3). We would be happy to include this graph in the manuscript should the reviewer agree.

761 There are several possible explanations for this

762 cell-specific difference:

763 1. Whilst PK4C9 showed low toxicity in fibroblasts 24 h after treatment (10.1% death at

764 40 μM), cytotoxicity was higher in HeLa and it increased with time (15.9% at 6 h *vs*.

765 23.5% at 24 h, at 40 μM). Toxicity could therefore explain that the splicing modifier effect

766 of PK4C9 decreases with time in HeLa but not in fibroblasts. (Note that we use "% of

767 death at 40 μM" instead of LD50 values, because cells did not reach >50 % death even

768 after curve saturation).

769 2. HeLa are cancer cells. Cancer cells are known to often overexpress transporters that

770 pump substances out of the cell, a mechanisms leading to drug resistance. This could

771 also explain why the splicing modifier effect of PK4C9 decreases with time in HeLa but

772 not in fibroblasts.

773 We have now **modified the text** to mention these points in the Fig 3a legend, which
774 reads as follows:

775 *"Note that PK4C9 and BJGF466 elicit maximal E7 inclusion at early time points, may be*
776 *due to progressive compound toxicity and/or to the molecules being secreted out of the*
777 *cell at later time points, as previously seen in cancer cells ()."*

778

779 **4. A time course (up to 72 hrs or longer) study in dose response format is needed**
780 **to make a confident statement about the cytotoxicity of these molecules. A 24 hr**
781 **cytotoxicity study as shown in Fig 3d is inadequate and a tad misleading although**
782 **it shows PK4C9 to be superior to the other tested molecules at one early timepoint**
783 **and at a given dose. Given that there are over 200 splicing events impacted by the**
784 **molecule a more thorough evaluation of cytotoxicity is warranted.**

785 For our previous version of the manuscript, 24 h cytotoxicity curves were obtained by the
786 LDH method for our screening hits NCI377363, PK4C9, BJGF466, and 288D. At this
787 time point, some of the molecules did not reach >50 % death, even after curve
788 saturation. Therefore their LD50 value could not be calculated. To be able to compare
789 the toxicity of these four hits, we represented the "% of death at 40 μM" and "the % of
790 death at the concentration of maximum activity", as shown in Fig. 3d. In our revised
791 version of the manuscript we have included our complete **cytotoxicity curves at 24 h**
792 (see **new Supp. Fig. S7**). In addition, and following the recommendation of the reviewer,
793 we have also expanded our cytotoxicity analysis to **72 h**. At this time point, the same
794 trend was observed, with two molecules still not reaching >50 % death, and PK4C9
795 being the least toxic of the four. 100 % death was not reached by any molecule at any
796 concentration.

797

798 **5a. In their RNA-Seq experiment the authors identified 290 transcripts with**
799 **modified splicing relative to DMSO. The scope of alternative splicing events**
800 **impacted by the compound may be an underestimate given that sequencing reads**
801 **could not unambiguously mapped on to full length transcripts. A more stringent**
802 **statistical assessment of the splicing changes and a rank ordering of the changes**
803 **based on significance would be very informative.**

804   To address the question raised by the reviewer, the following **exon junction analysis**

805   was performed. Exon junctions with read support only in the treated but not in the control

806   samples were analyzed. The majority (80.7%) of those junctions are not in

807   RefSeq/Ensembl annotations (see **Table below**). However, more than half of the

808   junctions are represented in the Intropolis database by both (55.4%) or one (39.3%) of

809   the two junction coordinates. Thus, there is sequencing evidence for most of the

810   junctions in already published RNASeq experiments, arguing against the concern that

811   the scope of alternative splicing events impacted by PK4C9 may be an underestimate.

812   Only 38 junctions (5.3%) detected in the treated but not in the control samples were not

813   observed elsewhere.

Numbers of junctions represented in Intropolis and RefSeq/Ensembl GTF exon annotation		
	Intropolis Database	**RefSeq/Ensembl GTF**
begin and end coordinates present	399 (55.4%)	3 (0.4%)
only begin coordinate present	138 (19.2%)	62 (8.6%)
only end coordinate present	145 (20.1%)	74 (10.3%)
begin and end coordinate not present	38 (5.3%)	581 (80.7%)
Sum	**720**	**720**

814   This **new analysis and table** have now been incorporated to our revised Supporting

815   Methods section.

816   **5b. Also, It would be good for the authors to clarify which of the splicing events**

817   **are due to rescue of SMN2 splicing and which may be resulting from non-specific**

818   **interactions of the compound with other RNA sequences or RNA secondary**

819   **structures, genome wide. Comparison of the RNA Seq profile of PK4C9 in wild**

820   **type versus SMA patient fibroblasts could offer insights on this front.**

821   **Alternatively, comparison to SMN overexpression / rescue or to Spinraza**

822   **treatment would be informative in this regard.**

823   Our RNA sequencing (RNA-seq) analysis detected 201 differentially spliced genes with

824   an absolute PSI (percent spliced in) >0.4 upon treatment of human SMA fibroblasts

825   (GM03813C) with PK4C9 (40 μM, 24 h). A series of studies in mice have previously

826   shown that reduction of SMN protein results in widespread splicing abnormalities, the

827   identity of which depends on the genetic model, experimental conditions, and tissue/cell

828   lines used. For example, the following numbers of dysregulated splicing events have

829   been reported in SMN-depleted mice cells: 145 (motor neurons)[12]; 252 (spinal cord,

830 post-symptomatic stage), 16 (spinal cord, pre-symptomatic stage)[13]; 104 (motor
831 neurons), 86 (white matter)[14]; 259 (spinal cord), 73 (brain), and 633 (kidney)[15]. It is
832 therefore not surprising that the recovery of SMN protein induced by PK4C9 in SMA
833 fibroblasts is coupled with a large number of splicing changes, which could represent the
834 reversal of at least part of such generalized splicing abnormalities and be of therapeutic
835 relevance. ~25% of the changes found in our RNAseq study affect genes altered in
836 previous reports in mice. However, a formal comparison between ours and these
837 previous results has not been conducted in our study, given that the identity of specific
838 exons and introns affected in SMN-depleted mouse nerve cells has been shown to not
839 translate to human SMA fibroblasts[12].

840 Besides PK4C9, there are only two other examples of *SMN2*-splicing modifying small
841 molecules in the literature for which RNA-seq data also exist, the chemical scaffolds of
842 which differ notably from PK4C9. In particular:

843 (1) Novartis: NVS-SM1 (100 nM). 35 differentially spliced genes with PSI>0.4 were
844 identified[10].

845 (2) Hoffmann-La Roche: SMN-C3 (500 nM). 13 differentially spliced genes with PSI>0.4
846 were identified[9].

847 In these two cases, the molecules tested were not direct hits from a chemical screen
848 (like PK4C9), but chemically optimized leads with maximized cellular potency (nM range)
849 and oral availability. A fair comparison of these two molecules with PK4C9 can therefore
850 not be made, since PK4C9 is still in the pre-optimization stage. However, we did find
851 three differentially spliced genes (*SMN2*, *SLC25A17*, and *VPS29*) in common between
852 the three studies (see **Venn Diagram** below), further supporting that at least some of all
853 PK4C9-induced splicing changes represent a positive consequence of SMN protein
854 rescue.
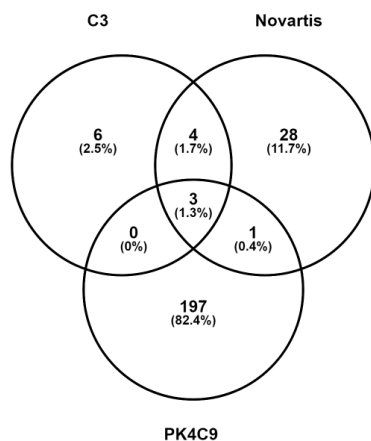
Venn diagram. Genes where alternative splicing events were detected with an absolute PSI of at least 0.4 between treated and control samples. There are three genes that were affected by all three compounds. http://bioinfogp.cnb.csic.es/tools/venny/index.html. We would be happy to include this figure in the manuscript should the reviewer agree

855 However, we acknowledge that part of the PK4C9-sensitive splicing changes are also
856 likely to be off-targets. In this regard, it is important to keep in mind that PK4C9, in its
857 current state, is not intended as a therapeutic agent, but as a proof-of-concept molecule
858 that will undergo chemical optimization to become a more potent and specific lead
859 compound. Being able to discern between undesired PK4C9-induced off-target *vs.* SMN
860 recovery-mediated splicing changes is key for the chemical optimization of PK4C9's
861 specificity. In an initial low-scale attempt, we compared the effect of PK4C9 on eight of
862 these genes in SMA *vs.* WT fibroblasts. To do this, we assumed that (1) true off-targets
863 would be similarly affected by PK4C9 in WT and SMA cells, but that (2) SMN-dependent
864 changes would respond differently to treatment in WT *vs.* SMA cells, given their different
865 SMN starting levels (see Fig. 4d). Four out of these eight genes belonged to the first
866 case and the remaining four to the second, confirming the co-existence of both effects.
867 We now plan to expand this analysis to the rest of transcripts and to combine this
868 information with our structural results (see Fig. 5, Fig. 6 and Fig. 7), in order to lead the
869 optimization of PK4C9's specificity.

870 Finally, the less-active, **structural analogues of PK4C9** that do not affect *SMN2* E7
871 inclusion (see **new Supp. Fig. S8**) also failed to modify the splicing of two of the
872 transcripts that we classified as SMN-recovery dependent, further validating our
873 conclusions.

874 **Mentions to all these points** have now been added to the Results and Discussion
875 sections of the revised version of our manuscript.

876

877 **6. The authors should seriously consider including a structurally related, inactive**
878 **(in SMN assays) compound as a negative control in their key cellular and**
879 **biophysical studies, NGS etc**

880 As requested by the reviewer, **eight structural analogues** of PK4C9 have been
881 generated and their TSL2-binding and functional data added to the manuscript (see **new**
882 **Supp. Fig. S8**). Compared to PK4C9, all these analogues displayed reduced binding to
883 TSL2 in our fluorescence displacement assay. This reduction was coupled with a
884 proportional loss of *SMN2* E7 splicing modifier activity in HeLa cells (*SMN2*[E6-7-8]
885 minigene) and SMA fibroblasts (endogenous *SMN2* transcript), which was in turn nicely
886 explained by their different binding poses found by molecular docking (see **new Supp.**

887   **Fig. S8**). Finally, the splicing of *LPIN1* and *RPS6KB1*, two transcripts found in our RNA-
888   seq analysis, the splicing changes of which were classified as SMN recovery-dependent,
889   were also not affected by the non-active PK4C9 analogues (see **new Supp. Fig. S8**).
890   Altogether, these results provide additional confirmation that the cellular activity of
891   PK4C9 is mediated by TSL2.

892

893   **7. In recent years there has been significant progress in identifying small**
894   **molecule and antisense-oligonucleotide based approaches to enhancing SMN2**
895   **splicing / exon 7 inclusion. Almost all of these approaches have relied on a couple**
896   **of mouse models of SMA to demonstrate in vivo efficacy. The current study**
897   **however provides evidence of in vivo efficacy in a less commonly used fly model**
898   **of SMA. This does not allow for proper benchmarking / comparison of TSL2**
899   **modulators to previously demonstrated approaches to enhancing SMN2 exon7**
900   **splicing that are currently in the clinic, which is critical given the current state of**
901   **the field.**

902   While we understand the point made by the reviewer, we would like to make the
903   following clarifications. We have also revised our manuscript text to clarify these points.

904

905   1. The *Drosophila* splicing sensor expresses a transgene with the human *SMN2* E6-7-8
906   sequence. PK4C9 was tested in this system to provide additional validation of its splicing
907   modifier activity, which in these flies can be easily and specifically targeted to motor
908   neurons. This validation was, however, not intended as a substitute of compound
909   evaluation in a mammalian SMA model, nor as proof of *in vivo* efficacy in the strict
910   sense. Indeed, the *Drosophila* splicing sensor cannot be considered an SMA disease
911   model, since these flies do not express pathogenic mutations.

912   2. Our study provides proof-of-concept to using small molecules to target TSL2 and
913   manipulate *SMN2* splicing, The hit molecules presented here are still in a pre-
914   optimization stage of development, and therefore we do not claim that they can be
915   considered as clinical candidates. However, we undertook an extensive effort to
916   describe and validate the mechanism of action of PK4C9, which would aid a subsequent
917   chemical optimization campaign for this molecule. It will be sensible that the subsequent
918   optimized lead compounds are assessed in the appropriate mice models, like the Smn

919 allele C[55] or the SMNdelta7[56]. However, we strongly believe that testing PK4C9 in its
920 current state on SMA mice models would have been a non-justifiable use of resources
921 and animals, which given the animal experimentation legislation in Switzerland would
922 have most likely lead to a negative cost benefit analysis. Specifically, the SMNdelta7 is a
923 severe disease model, where animals of the relevant genotype have to be generated for
924 every experiment by genetic crossing. These animals are extremely ill and die within ~2
925 weeks from birth, making their generation to evaluate a non-optimized hit, for which we
926 also do not have PK or *in vivo* distribution data, unjustifiable.

927

928 **8. While Garcia-Lopez et al present promising, early evidence for the identification**
929 **of small molecule modulators of the TSL2 stem loop structure in SMN2 the study**
930 **fails to provide thorough validation and selectivity assessment of the**
931 **compound(s). The current study represents a modest, incremental increase in our**
932 **structural and mechanistic understanding of how TSL2 (which has long been**
933 **known to be a key regulatory region for SMN2 splicing) may be modulated with**
934 **small molecules to enhance SMN2 exon 7 inclusion. In summary, I would not**
935 **recommend accepting this manuscript for publication in its current form.**

936 We hope to have provided enough convincing data and arguments to address the
937 concerns of the reviewer, and to have presented the strengths of our study more clearly
938 in our revised version of the manuscript , as well as throughout this document.

939

940

941

942

943

944

945

946

947

948

References

1. Furtig, B., *et al.* Time-resolved NMR studies of RNA folding. *Biopolymers* **86**, 360-383 (2007).
2. Singh, N.N., Singh, R.N. & Androphy, E.J. Modulating role of RNA structure in alternative splicing of a critical exon in the spinal muscular atrophy genes. *Nucleic Acids Res* **35**, 371-389 (2007).
3. Burd, C.G. & Dreyfuss, G. RNA binding specificity of hnRNP A1: significance of hnRNP A1 high-affinity binding sites in pre-mRNA splicing. *EMBO J* **13**, 1197-1204 (1994).
4. Brichta, L., *et al.* Valproic acid increases the SMN2 protein level: a well-known drug as a potential therapy for spinal muscular atrophy. *Human molecular genetics* **12**, 2481-2489 (2003).
5. Hofmann, Y., Lorson, C.L., Stamm, S., Androphy, E.J. & Wirth, B. Htra2-beta 1 stimulates an exonic splicing enhancer and can restore full-length SMN expression to survival motor neuron 2 (SMN2). *Proc Natl Acad Sci U S A* **97**, 9618-9623 (2000).
6. Cartegni, L., Hastings, M.L., Calarco, J.A., de Stanchina, E. & Krainer, A.R. Determinants of exon 7 splicing in the spinal muscular atrophy genes, SMN1 and SMN2. *Am J Hum Genet* **78**, 63-77 (2006).
7. Zhang, M.L., Lorson, C.L., Androphy, E.J. & Zhou, J. An in vivo reporter system for measuring increased inclusion of exon 7 in SMN2 mRNA: potential therapy of SMA. *Gene therapy* **8**, 1532-1538 (2001).
8. Mayer, F., *et al.* Evolutionary conservation of vertebrate blood-brain barrier chemoprotective mechanisms in Drosophila. *J Neurosci* **29**, 3538-3550 (2009).
9. Naryshkin, N.A., *et al.* Motor neuron disease. SMN2 splicing modifiers improve motor function and longevity in mice with spinal muscular atrophy. *Science* **345**, 688-693 (2014).
10. Palacino, J., *et al.* SMN2 splice modulators enhance U1-pre-mRNA association and rescue SMA mice. *Nature chemical biology* **11**, 511-517 (2015).
11. Grzeschik, S.M., Ganta, M., Prior, T.W., Heavlin, W.D. & Wang, C.H. Hydroxyurea enhances SMN2 gene expression in spinal muscular atrophy cells. *Ann Neurol* **58**, 194-202 (2005).
12. Custer, S.K., *et al.* Altered mRNA Splicing in SMN-Depleted Motor Neuron-Like Cells. *PloS one* **11**, e0163954 (2016).
13. Baumer, D., *et al.* Alternative splicing events are a late feature of pathology in a mouse model of spinal muscular atrophy. *PLoS Genet* **5**, e1000773 (2009).
14. Zhang, Z., *et al.* Dysregulation of synaptogenesis genes antecedes motor neuron pathology in spinal muscular atrophy. *Proc Natl Acad Sci U S A* **110**, 19348-19353 (2013).
15. Zhang, Z., *et al.* SMN deficiency causes tissue-specific perturbations in the repertoire of snRNAs and widespread defects in splicing. *Cell* **133**, 585-600 (2008).
16. Underwood, J.G., *et al.* FragSeq: transcriptome-wide RNA structure probing using high-throughput sequencing. *Nat Methods* **7**, 995-1001 (2010).

994   17.   Siegfried, N.A., Busan, S., Rice, G.M., Nelson, J.A. & Weeks, K.M. RNA motif
995   discovery by SHAPE and mutational profiling (SHAPE-MaP). *Nat Methods* **11**,
996   959-965 (2014).
997   18.   Zubradt, M.*, et al.* DMS-MaPseq for genome-wide or targeted RNA structure
998   probing in vivo. *Nat Methods* **14**, 75-82 (2017).
999   19.   Singh, N.N., Lee, B.M. & Singh, R.N. Splicing regulation in spinal muscular
1000   atrophy by an RNA structure formed by long-distance interactions. *Annals of
1001   the New York Academy of Sciences* **1341**, 176-187 (2015).
1002 20.   Kulik, M., Goral, A.M., Jasinski, M., Dominiak, P.M. & Trylska, J. Electrostatic
1003   interactions in aminoglycoside-RNA complexes. *Biophysical journal* **108**, 655-
1004   665 (2015).
1005 21.   Meiler, J. PROSHIFT: protein chemical shift prediction using artificial neural
1006   networks. *J Biomol NMR* **26**, 25-37 (2003).
1007 22.   Han, B., Liu, Y., Ginzinger, S.W. & Wishart, D.S. SHIFTX2: significantly
1008   improved protein chemical shift prediction. *J Biomol NMR* **50**, 43-57 (2011).
1009 23.   Xu, X.P. & Case, D.A. Automated prediction of 15N, 13Calpha, 13Cbeta and
1010   13C' chemical shifts in proteins using a density functional database. *J Biomol
1011   NMR* **21**, 321-333 (2001).
1012 24.   Kohlhoff, K.J., Robustelli, P., Cavalli, A., Salvatella, X. & Vendruscolo, M. Fast
1013   and accurate predictions of protein NMR chemical shifts from interatomic
1014   distances. *J Am Chem Soc* **131**, 13894-13895 (2009).
1015 25.   Atieh, Z., Aubert-Frecon, M. & Allouche, A.R. Rapid, accurate and simple
1016   model to predict NMR chemical shifts for biological molecules. *J Phys Chem B*
1017   **114**, 16388-16392 (2010).
1018 26.   Shen, Y. & Bax, A. SPARTA+: a modest improvement in empirical NMR
1019   chemical shift prediction by means of an artificial neural network. *J Biomol
1020   NMR* **48**, 13-22 (2010).
1021 27.   Cromsigt, J.A., Hilbers, C.W. & Wijmenga, S.S. Prediction of proton chemical
1022   shifts in RNA. Their use in structure refinement and validation. *J Biomol NMR*
1023   **21**, 11-29 (2001).
1024 28.   Dejaegere, A., Bryce, R.A. & A., C.D. An Empirical Analysis of Proton Chemical
1025   Shifts in Nucleic Acids. *ACS Symp. Ser.* **732**, 194–206 (1999).
1026 29.   Lange, O.F., van der Spoel, D. & de Groot, B.L. Scrutinizing molecular
1027   mechanics force fields on the submicrosecond timescale with NMR data.
1028   *Biophysical journal* **99**, 647-655 (2010).
1029 30.   Dalvit, C.*, et al.* Identification of compounds with binding affinity to proteins
1030   via magnetization transfer from bulk water. *J Biomol NMR* **18**, 65-68 (2000).
1031 31.   Muller, C.W., Schlauderer, G.J., Reinstein, J. & Schulz, G.E. Adenylate kinase
1032   motions during catalysis: an energetic counterweight balancing substrate
1033   binding. *Structure* **4**, 147-156 (1996).
1034 32.   Silvers, R., Keller, H., Schwalbe, H. & Hengesbach, M. Differential scanning
1035   fluorimetry for monitoring RNA stability. *Chembiochem : a European journal
1036   of chemical biology* **16**, 1109-1114 (2015).
1037 33.   Orry, A.J., Abagyan, R.A. & Cavasotto, C.N. Structure-based development of
1038   target-specific compound libraries. *Drug discovery today* **11**, 261-266 (2006).

1039 34. Harris, C.J., Hill, R.D., Sheppard, D.W., Slater, M.J. & Stouten, P.F. The design
1040   and application of target-focused compound libraries. *Comb Chem High*
1041   *Throughput Screen* **14**, 521-531 (2011).
1042 35. Tran, T. & Disney, M.D. Identifying the preferred RNA motifs and chemotypes
1043   that interact by probing millions of combinations. *Nature communications* **3**,
1044   1125 (2012).
1045 36. Thomas, J.R. & Hergenrother, P.J. Targeting RNA with small molecules. *Chem*
1046   *Rev* **108**, 1171-1224 (2008).
1047 37. Bodoor, K.*, et al.* Design and implementation of an ribonucleic acid (RNA)
1048   directed fragment library. *J Med Chem* **52**, 3753-3761 (2009).
1049 38. Maly, D.J., Choong, I.C. & Ellman, J.A. Combinatorial target-guided ligand
1050   assembly: identification of potent subtype-selective c-Src inhibitors. *Proc*
1051   *Natl Acad Sci U S A* **97**, 2419-2424 (2000).
1052 39. Kralovicova, J., Patel, A., Searle, M. & Vorechovsky, I. The role of short RNA
1053   loops in recognition of a single-hairpin exon derived from a mammalian-wide
1054   interspersed repeat. *RNA Biol* **12**, 54-69 (2015).
1055 40. Disney, M.D., Yildirim, I. & Childs-Disney, J.L. Methods to enable the design of
1056   bioactive small molecules targeting RNA. *Org Biomol Chem* **12**, 1029-1039
1057   (2014).
1058 41. Guan, L. & Disney, M.D. Recent advances in developing small molecules
1059   targeting RNA. *ACS chemical biology* **7**, 73-86 (2012).
1060 42. Disney, M.D. Rational design of chemical genetic probes of RNA function and
1061   lead therapeutics targeting repeating transcripts. *Drug discovery today*
1062   (2013).
1063 43. Gareiss, P.C.*, et al.* Dynamic combinatorial selection of molecules capable of
1064   inhibiting the (CUG) repeat RNA-MBNL1 interaction in vitro: discovery of
1065   lead compounds targeting myotonic dystrophy (DM1). *J Am Chem Soc* **130**,
1066   16254-16261 (2008).
1067 44. Warf, M.B., Nakamori, M., Matthys, C.M., Thornton, C.A. & Berglund, J.A.
1068   Pentamidine reverses the splicing defects associated with myotonic
1069   dystrophy. *Proc Natl Acad Sci U S A* **106**, 18551-18556 (2009).
1070 45. Velagapudi, S.P.*, et al.* Design of a small molecule against an oncogenic
1071   noncoding RNA. *Proc Natl Acad Sci U S A* **113**, 5898-5903 (2016).
1072 46. Stelzer, A.C.*, et al.* Discovery of selective bioactive small molecules by
1073   targeting an RNA dynamic ensemble. *Nature chemical biology* **7**, 553-559
1074   (2011).
1075 47. Patwardhan, N.N.*, et al.* Amiloride as a new RNA-binding scaffold with
1076   activity against HIV-1 TAR. *Medchemcomm* **8**, 1022-1036 (2017).
1077 48. Velagapudi, S.P. & Disney, M.D. Two-dimensional combinatorial screening
1078   enables the bottom-up design of a microRNA-10b inhibitor. *Chem Commun*
1079   *(Camb)* **50**, 3027-3029 (2014).
1080 49. Di Giorgio, A., Tran, T.P. & Duca, M. Small-molecule approaches toward the
1081   targeting of oncogenic miRNAs: roadmap for the discovery of RNA
1082   modulators. *Future Med Chem* **8**, 803-816 (2016).

1083   50.   Luo, Y. & Disney, M.D. Bottom-up design of small molecules that stimulate
1084   exon 10 skipping in mutant MAPT pre-mRNA. *Chembiochem : a European*
1085   *journal of chemical biology* **15**, 2041-2044 (2014).
1086   51.   Liu, Y., Rodriguez, L. & Wolfe, M.S. Template-directed synthesis of a small
1087   molecule-antisense conjugate targeting an mRNA structure. *Bioorg Chem* **54**,
1088   7-11 (2014).
1089   52.   Reichert, C., Perozzo, R. & Borchard, G. Non-covalent modification of
1090   granulocyte-colony stimulating factor (G-CSF) by coiled-coil technology. *Int J*
1091   *Pharm* **511**, 98-103 (2016).
1092   53.   Perozzo, R., Folkers, G. & Scapozza, L. Thermodynamics of protein-ligand
1093   interactions: history, presence, and future aspects. *J Recept Signal Transduct*
1094   *Res* **24**, 1-52 (2004).
1095   54.   Seeliger, M.A.*, et al.* c-Src binds to the cancer drug imatinib with an inactive
1096   Abl/c-Kit conformation and a distributed thermodynamic penalty. *Structure*
1097   **15**, 299-311 (2007).
1098   55.   Osborne, M.A.*, et al.* Characterization of behavioral and neuromuscular junction
1099   phenotypes in a novel allelic series of SMA mouse models. *Human molecular*
1100   *genetics* **21**, 4431-4447 (2012).
1101   56.   Le, T.T.*, et al.* SMNDelta7, the major product of the centromeric survival
1102   motor neuron (SMN2) gene, extends survival in mice with spinal muscular
1103   atrophy and associates with full-length SMN. *Human molecular genetics* **14**,
1104   845-857 (2005).

Reviewers' Comments:

Reviewer #1:
Remarks to the Author:
The authors have replied to most of my comments satisfactorily.
However I would like to make a couple of comments regarding the replies (numbering as in the original review):

1- It would have been nice that the RT-PCR gel consistent with the bar graph was already there in the first version.

6- My experience with these techniques contradicts partially the author's statement: "qPCR has higher sensitivity and reliability over a greater dynamic range of RNA concentrations than other techniques, including semi-quantitative PCR or Northern blot." While there is no doubt about higher sensitivity of PCR methods, Northern blots are far more reliable than qPCR because, not depending on amplification methods, are more representative of the real mRNA concentrations in the cell/tissue. The fact that the authors do not have access to radioactive nucleotides is understandable but does not justify such sweeping statement.

Reviewer #2:
Remarks to the Author:
The new experiments and discussion clearly add to the contribution of this paper, and all of my concerns from my previous review have been addressed. I recommend an accept.

Reviewer #3:
Remarks to the Author:
No further revisions are required. Proposed changes & explanation were sufficient and the manuscript can be accepted.

Reviewer #5:
Remarks to the Author:
The concerns raised by all the reviewers were thoroughly addressed by the authors. Additional experiments were performed and corrections to the manuscript were made. Regarding the issues raised by Reviewer 4:
1) The authors provide sufficient evidence for the significance of the study. Specifically, the influence of triloop and pentaloop conformations of TSL2 on E7 splicing and the first NMR structure of TSL2. These contributions can aid in the further development of small molecules in the treatment of SMA and can be extrapolated to other splicing-mediated diseases targeting RNA.
2) Regarding the selectivity of binding of PK4C9 to TSL2 the authors demonstrate that the compound does not bind to unrelated RNA used in their study (Supple Fig S6).
3) The concern regarding the metal ion contaminants causing a change in the TSL2 conformation were appropriately addressed by carrying out elemental analysis of PK4C9 sample, which showed presence of metals (Pd, Mg, Fe) in trace quantities. Also, the use of 0.1 mM EDTA as a metal chelator in the NMR buffer ruled out the possibility of conformational change attributed to the presence of metal ions.
4) The shift in the compound spectra on binding to TSL2 was demonstrated by WaterLOGSY experiment.
5) An attempt to conduct direct binding assays was done by using SPR and ITC assays. However, due to weak binding affinity and solubility issues, these experiments were not conducted at higher

concentrations to determine the Kd value. In addition, the authors conducted fluorescent displacement assay with Ribogreen dye to rule out a false positive obtained by using TO-PRO1 dye.

6) Regarding the dose responsiveness of PK4C9, the text was appropriately modified in the legend for Fig 3.

7) Similarly, the maximal E7 inclusion at early time point observed in case of PK4C9 and BJGF466 in HeLa cells was attributed to higher toxicity of these compounds in HeLa cells lines compared to fibroblasts and presence of transporters in HeLa cells that pump out compounds from the cells. The text was modified in the legend for Fig 3a.

8) Cytotoxicity analysis up to 72 hours was performed as suggested by the reviewer.

9) To confirm that the activity of PK4C9 was mediated by binding to TSL2, eight additional analogs of PK4C9 were tested to correlate the TSL2 binding with the % E7 inclusion.

10) The authors suggested that the studies with PK4C9 were proof-of-concept studies and the molecule was not intended to be used as a therapeutic compound. Due to this reason, the authors did not test PK4C9 in mice models of the disease.

11) I find it most concerning that a Kd of 150-200- uM is found for the compound and yet the cellular act ivy is 10-fold lower concentration. Does this not argue for activity being due to non-specific effects. this must be addressed

We thank all Reviewers for their time and positive feedback. We include responses to the minor points of Reviewer 1 and 5 below. Changes in the manuscript have been highlighted in yellow. We trust that the Reviewers will now find our manuscript suitable for publication, as already agreed by Reviewer 2 and 3.

Reviewer #1

The authors have replied to most of my comments satisfactorily. However I would like to make a couple of comments regarding the replies (numbering as in the original review):

1) It would have been nice that the RT-PCR gel consistent with the bar graph was already there in the first version.

We agree with the Reviewer and we apologize for not having shown a better image in our first version of the manuscript to represent the 8 replicates (3 biological and 2-3 technical) quantified in Fig 1c.

6) My experience with these techniques contradicts partially the author's statement: "qPCR has higher sensitivity and reliability over a greater dynamic range of RNA concentrations than other techniques, including semi-quantitative PCR or Northern blot." While there is no doubt about higher sensitivity of PCR methods, Northern blots are far more reliable than qPCR because, not depending on amplification methods, are more representative of the real mRNA concentrations in the cell/tissue. The fact that the authors do not have access to radioactive nucleotides is understandable but does not justify such sweeping statement.

We apologize for our unfortunate wording. It was not our intention to question the reliability of Northern blot, as we are aware of the advantages of this technique, including the direct visualization of RNA bands. Our statement referred to the potentially wider range of RNA concentrations that can be quantified by qPCR. The following **text** has now been included to the Materials and Methods section of our manuscript (**page 18**) to complement the point raised by the Reviewer: *"qPCR. […]. Due to the low copy number of SMN2 transcripts, non-radioactive Northern blot failed to show visible SMN2 bands and could not be used as a validation technique. SMN2 isoform bands were shown by semi-quantitative PCR instead".*

Reviewer #5:

The concerns raised by all the reviewers were thoroughly addressed by the authors. Additional experiments were performed and corrections to the manuscript were made. Regarding the issues raised by Reviewer 4

[Points 1-10 removed as these were addressed]

11) I find it most concerning that a Kd of 150-200- uM is found for the compound and yet the cellular activity is 10-fold lower concentration. Does this not argue for activity being due to non-specific effects. this must be addressed.

First, we thank Reviewer #5 for their time assessing our response to Reviewer's #4 comments and for acknowledging our efforts in this regard. With respect to comment 11, we find it unlikely that activity is due to non-specific effects, as there are other more plausible explanations for the mismatch between the predicted Kd and cellular activity, detailed in points 1-3 below.

(1) We have shown that the effect of PK4C9 on *SMN2* E7 inclusion depends on the

structural integrity of TSL2 (Fig. 5 b, c). Moreover, we were able to link the effect of PK4C9 on E7 inclusion to TSL2 binding efficiency by studying eight structural analogues of this compound (Supp. Fig. S8). These observations demonstrate that the splicing modifier activity of PK4C9 is mediated by TSL2 and argue against an off-target as the responsible for the observed *SMN2* splicing changes.

(2) The EC50 value of PK4C9 in our splicing cellular assay is ~25 μM. Consistently, the EC50 value of PK4C9 in our TO-PRO-1 binding assay is 16 μM (Fig. 2c). Despite our efforts, ITC failed to provide an experimentally calculated Kd value for PK4C9, and an <u>estimated</u> Kd of 100-200 μM (which is ~3.5-to-7 times higher than the cellular EC50) was proposed. However, this Kd value may be an underestimate, given the poor solubility of PK4C9 in ITC buffer, which could lead to invisible precipitation of the compound and a reduction of its real concentration in solution. It is likely that the solubility of PK4C9 in TO-PRO-1 assay buffer and cell culture medium is better than in ITC buffer, which would increase the percentage of PK4C9 molecules available to reach TSL2.

(3) The ratio between folded and unfolded TSL2 states likely differs in vitro and in vivo due to molecular-crowding effects. Molecular crowding tends to favor the folded state of RNA inside the cell compared to in vitro conditions, which could influence target recognition[1]. Moreover, our cellular and ITC assays measure different things (namely, splicing and binding, respectively). In cells, the extent and lifetime of the conformational effect of PK4C9 on TSL2 may be sufficient to promote the downstream splicing effect, despite the low predicted Kd of the compound in vitro[2].

Because of its <u>estimated</u> nature, and given the above points, the Kd value proposed by ITC was given in our answer to Reviewer #4 but was not included in the main text of our manuscript. However, in reference to the point raised by Reviewer #5, the following **text** has now been included to the Results section of our manuscript (**page 7**): *"(PK4C9) showed the strongest effect, with an average E7 inclusion of up to 72% at 40 μM (43% increase respect to DMSO-treated cells) corresponding to an EC50 value of ~25 μM that is consistent with the EC50 value of PK4C9 in the TO-PRO-1 binding assay (16 μM, Fig. 2c)"*. We hope that our explanations and text modification have addressed the concern of the Reviewer satisfactorily.

1.   Dupuis, N.F., Holmstrom, E.D. & Nesbitt, D.J. Molecular-crowding effects on single-molecule RNA folding/unfolding thermodynamics and kinetics. *Proc Natl Acad Sci U S A* **111**, 8464-8469 (2014).
2.   Copeland, R.A., Pompliano, D.L. & Meek, T.D. Drug-target residence time and its implications for lead optimization. *Nature reviews. Drug discovery* **5**, 730-739 (2006).